Image Cover Sheet

CLASSIFICATION	SYSTEM NUMBER
UNCLASSIFIED	516903

TITLE

Investigation of plastic zone development in dynamic tear test specimens - Phase III

System Number:

Patron Number:

Requester:

Notes:

DSIS Use only:

Deliver to: CL

This page is left blank

This page is left blank

Copy No: 16

DEFENCE R&D DÉFENSE

Investigation of Plastic Zone Development in Dynamic Tear Test Specimens - Phase III

T S Koko and B K Gallant

Martec Limited
400-1888 Brunswick Street
Halifax, Nova Scotia, Canada
B3J 3J8

Contract #W7707-0-8440

Defence R&D Canada

Contractor Report
DREA CR 2001-121
September 2001

National Defence Défense nationale

Canada

REPRODUCTION QUALITY NOTICE

This document is the best quality available. The copy furnished to DRDCIM contained pages that may have the following quality problems:

: Pages smaller or Larger than normal

: Pages with background colour or light coloured printing

: Pages with small type or poor printing; and or

: Pages with continuous tone material or colour photographs

Due to various output media available these conditions may or may not cause poor legibility in the hardcopy output you receive.

☒ If this block is checked, the copy furnished to DRDCIM contained pages with colour printing, that when reproduced in Black and White, may change detail of the original copy.

Copy No: _____

INVESTIGATION OF PLASTIC ZONE DEVELOPMENT IN DYNAMIC TEAR TEST SPECIMENS - PHASE III

T.S. Koko and B.K. Gallant

Martec Limited
400 – 1888 Brunswick Street
Halifax, Nova Scotia, Canada
B3J 3J8

W7707-0-8440
Contract Number

Defence Research Establishment Atlantic

Contractor Report

DREA CR 2001-121

2001-09-21

Approved by

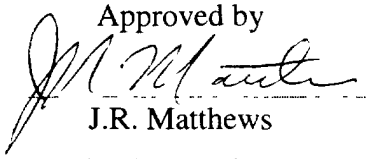

J.R. Matthews

Scientific Authority

Approved for release by

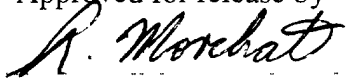

R.M.Morchat

H/DL(A)

The scientific or technical validity of this Contract Report is entirely the responsibility of the contractor and the contents do not necessarily have the approval or endorsement of Defence R&D Canada

Abstract

This study is a continuation of efforts to investigate plastic zone development in three-point bend fracture specimens to provide an understanding of crack tip blunting (stretch zone) to plastic zone size (radius), in order to be able to predict the upper limit where elastic plastic fracture becomes invalid Finite element analyses of an 8 mm specimen made of 350WT steel were performed with the aim of investigating the effects of various modeling (mesh) parameters on the behaviour of 2-D finite element models; and 3-D modeling to investigate shear lip behaviour. The ABAQUS finite element code was used to perform incremental elastic-plastic analysis of the specimens. The results computed included the progression of plastic strain, plastic radius (r_y), stretch zone width (SZW), and the r_y/SZW ratio with plastic displacement. It was found that the plastic radius and maximum plastic strains were not too sensitive to the mesh size around the crack tip, whereas the SZW is highly sensitive to mesh size around the crack tip. Thus the r_y/SZW ratio also depends on mesh configuration. In creating meshes around the tip, it is necessary to ensure that the sizes of the elements around the tip are such that several elements are contained in the region from the crack tip to the side of the crack where the yield line intersects the side of the crack. The 3-D analyses confirmed the in-plane plastic zone patterns obtained from the 2-D analyses and provided some insight on the shear lip behaviour However, the results obtained from the analyses did not provide a distinct point at which to measure the shear lip. At a plastic displacement of 0.0975B

(B = specimen thickness) the shear index was estimated to be 0.6 at the point where the yield lines were closest. Further studies are required to provide more accurate estimates of the shear lip size

Résumé

La présente étude s'inscrit dans la foulée des efforts visant à étudier le développement d'une zone plastique dans des éprouvettes soumises à des essais de pliage et comportant une fissure à trois inflexions, afin de mieux comprendre l'arrondissement de l'extrémité de fissure (zone d'allongement) par rapport aux dimensions de la zone plastique (rayon), dans le but de prévoir la limite supérieure à laquelle la fissure plastique élastique n'est plus valide. Des analyses par éléments finis d'une éprouvette de 8 mm en acier 350WT ont été réalisées dans le but d'étudier les effets des différents paramètres de modélisation (mailles) sur le comportement des modèles 2D à éléments finis; et l'on a procédé à la modélisation 3D en vue d'étudier le comportement de l'arête de cisaillement. Le programme à éléments finis ABAQUS a été utilisé pour effectuer une analyse plastique-élastique différentielle des éprouvettes. Les résultats calculés comprenaient la progression de la déformation plastique, du rayon plastique (r_y), de la largeur de la zone d'allongement (SZW), et du rapport r_y/SZW en fonction du déplacement plastique. On a déterminé que le rayon plastique et les déformations plastiques maximales n'*étaient* pas trop sensibles à la taille des mailles autour de l'extrémité de fissure, alors que la SZW est très sensible à la taille des mailles autour de l'extrémité de fissure. Ainsi, le rapport r_y/SZW dépend également de la configuration des mailles. En créant des mailles autour de l'extrémité, il est nécessaire de s'assurer que les dimensions des éléments autour de l'extrémité sont telles que plusieurs éléments sont contenus dans la zone commençant à l'extrémité de fissure et allant jusqu'au côté de la fissure où la ligne formée des points

correspondant à la limite d'élasticité apparente (ligne d'élasticité) rencontre le côté de la fissure. Les analyses 3D ont permis d'obtenir une confirmation des modèles de zone plastique dans un plan obtenus dans les analyses 2D et donnent un aperçu du comportement de l'arête de cisaillement. Cependant, les résultats obtenus dans les analyses n'ont pas permis de déterminer un point distinct auquel mesurer l'arête de cisaillement. Pour un déplacement plastique de 0,0975B (B = épaisseur de l'éprouvette), l'indice de cisaillement a été estimé à 0,6 au point où les lignes d'élasticité étaient le plus rapprochées. D'autres études sont requises pour obtenir des estimations plus précises des dimensions de l'arête de cisaillement.

Executive summary

This study is a continuation of efforts to investigate plastic zone development in three-point bend fracture specimens using 3D finite element technology. This will provide an understanding of crack tip blunting (stretch zone) to plastic zone size (radius), which is needed in order to be able to predict the upper limit where elastic plastic fracture becomes invalid. Finite element analyses were performed with the aim of investigating the effects of various modeling (mesh) parameters on the behaviour of 2-D finite element models; and 3-D modeling to investigate shear lip behaviour. The ABAQUS finite element code was used. The results computed included the progression of plastic strain, plastic radius (r_y), stretch zone width (SZW), and the r_y/SZW ratio with plastic displacement.

It was found that the plastic radius and maximum plastic strains were not too sensitive to the mesh size around the crack tip, whereas the SZW is highly sensitive to mesh size around the crack tip. Thus the r_y/SZW ratio also depends on mesh configuration. In creating meshes around the tip, it is necessary to ensure that the sizes of the elements around the tip are such that several elements are contained in the region from the crack tip to the side of the crack where the yield line intersects the side of the crack The 3-D analyses confirmed the in-plane plastic zone patterns obtained from the 2-D analyses and provided some insight on the shear lip behaviour. However, the results obtained from the analyses did not provide a distinct point at which to measure the shear lip At a plastic displacement of 0.0975B (B = specimen thickness) the shear index was estimated to be 0.6 at the point where the yield lines were closest

Further studies are required to provide more accurate estimates of the shear lip size. Several new contracts aimed at modeling developing shear lips are planned.

Koko, T S and Gallant, B K., 2001 Investigation of Plastic Zone Development in Dynamic Tear Test Specimens-Phase III, DREA CR 2001-121, Defence Research Establishment Atlantic

Sommaire

La présente étude s'inscrit dans la foulée des efforts visant à étudier le développement d'une zone plastique dans des éprouvettes soumises à des essais de pliage et comportant une fissure à trois inflexions, à l'aide d'une technologie par éléments finis 3D. Elle permettra de mieux comprendre l'arrondissement de l'extrémité de fissure (zone d'allongement) par rapport aux dimensions de la zone plastique (rayon), dans le but de prévoir la limite supérieure à laquelle la fissure plastique élastique n'est plus valide. Des analyses par éléments finis ont été effectuées dans le but d'étudier les effets de différents paramètres de modélisation (mailles) sur le comportement des modèles à éléments finis 2D; et l'on a procédé à la modélisation 3D en vue d'étudier le comportement de l'arête de cisaillement. Le programme à éléments finis ABAQUS a été utilisé. Les résultats calculés comprenaient la progression de la déformation plastique, du rayon plastique (r_y), de la largeur de la zone d'allongement (SZW), et du rapport r_y/SZW en fonction du déplacement plastique.

On a déterminé que le rayon plastique et les déformations plastiques maximales n'étaient pas trop sensibles à la taille des mailles autour de l'extrémité de fissure, alors que la SZW est très sensible à la taille des mailles autour de l'extrémité de fissure. Ainsi, le rapport r_y/SZW dépend également de la configuration des mailles. En créant des mailles autour de l'extrémité, il est nécessaire de s'assurer que les dimensions des éléments autour de l'extrémité sont telles que plusieurs éléments sont contenus dans la zone commençant à l'extrémité de fissure et allant jusqu'au côté de la fissure où la ligne formée des points correspondant à la limite d'élasticité apparente (ligne d'élasticité) rencontre le côté de la fissure. Les analyses 3D ont permis d'obtenir une confirmation des modèles de zone plastique dans un plan obtenus dans les analyses 2D et donnent un aperçu du comportement de l'arête de cisaillement. Cependant, les résultats obtenus dans les analyses n'ont pas permis de déterminer un point distinct auquel mesurer l'arête de cisaillement. Pour un déplacement plastique de 0,0975B (B = épaisseur de l'éprouvette), l'indice de cisaillement a été estimé à 0,6 au point où les lignes d'élasticité étaient le plus rapprochées

D'autres études sont requises pour obtenir des estimations plus précises des dimensions de l'arête de cisaillement. Plusieurs nouveaux contrats portant sur l'élaboration de modèles d'arêtes de cisaillement sont prévus.

Koko, T.S et Gallant, B.K , 2001 *Investigation of Plastic Zone Development in Dynamic Tear Test Specimens-Phase III*, CRDA CR 2001-121, Centre de recherches pour la défense – Atlantique

Acknowledgements

The authors would like to acknowledge the contributions of Dr. E.C. Oguejiofor of St. Francis Xavier University, Antigonish, NS and Mr. Tim Dunbar of Martec Limited, Halifax, NS.

TABLE OF CONTENTS

LIST OF FIGURES

1. INTRODUCTION

1.1 Background

This study is the Phase III of an effort [1,2] to provide an understanding of the ratio of crack tip blunting (stretch zone) to the plastic zone size (radius) in order to determine the upper limit of temperature relative to full size transition curves where elastic plastic fracture becomes invalid. The finite element (FE) technique is used to provide this ratio and the result of interest is the development of the plastic zone in dynamic tear (DT) type test specimens. The dynamic tear test involves a single-edge notched beam that is loaded in three-point bending. The size and shape of the plastic zone, the stretch zone and the shear lips that form are important parameters that can be used to develop analytical models for describing the material behaviour.

In the Phase II study [2], 2-D finite element analysis was utilized to provide an understanding of the plastic zone size (radius) to crack tip blunting (stretch zone width) for 350WT steel and 304 stainless steel specimens. For each type of material, three geometric configurations were considered to study the effect of specimen size. The ABAQUS finite element code was used to perform incremental elastic-plastic analysis of the specimens. Refined stress-strain curves for the 350WT and 304 stainless steel materials beyond the limits of uni-axial stress-strain data were obtained from experimental investigations at DREA and utilized to model the constitutive behaviour. Results computed included the midpoint displacement; development of the plastic zone around the crack tip with progression of load; the plastic zone radius r_y; stretch zone width (SZW); and the ratio of plastic zone radius to SZW. The results were presented in the form of contour plots and charts. The goal of the present study is to continue the Phase II work in order to provide better accuracy and to provide further insight into the fracture behaviour of the materials.

1.2 Objectives and Scope

The specific objectives of the present study include (i) to investigate the effect of various modeling (mesh) parameters on the behaviour of the 2-D finite element models; and (ii) to perform 3-D analysis of the DT specimens, in order to investigate the shear-lip behaviour.

Chapter 2 provides descriptions of the specimen configurations considered in the study. The finite element methodology utilized in the investigation is presented in Chapter 3 and the results are presented in Chapter 4. Finally, Chapter 5 provides a summary of the study and the conclusions reached.

2. PROBLEM DESCRIPTION

2.1 Specimen Configurations

A schematic representation of the test specimen is presented in Figure 2.1. In the present study, two test configurations are analyzed. These include the following:

(i) DT specimen, 350WT material, 8 mm thickness (designated as DT-350WT-08); and
(ii) NS specimen, 350WT material, 2 mm thickness (designated as NS-350WT-02).

The dimensions of the specimens are shown in Table 2.1. The crack tip shape is that of a fatigue crack initially and a blunted fatigue crack thereafter, as described in [1,2].

2.2 Requirements

It was required to compute the progression of the plastic zone around the crack tip under quasi-static loading conditions, for the three specimens. The following specific analyses are required:

(i) 2-D analysis of DT-350WT-08 specimen with the mesh used in Phase II [2] but with quadratic elements
(ii) 2-D analysis of DT-350WT-08 specimen with more refined mesh, using linear elements and (b) quadratic elements;
(iii) 2-D analysis of DT-350WT-08 specimen with coarser mesh, using (a) linear elements and (b) quadratic elements;
(iv) 3-D analysis of DT-350WT-08 specimen, using suitable mesh configuration; and
(v) 3-D analysis of DT-350WT-02 specimen, using suitable mesh configuration

Analysis results of interest include:

(i) Progression of plastic zone around the crack tip, including contour plots of plastic strain;
(ii) Midpoint plastic deflections;
(iii) Stretch zone width (i.e. distance from crack tip to interface of yield zone with side of crack);
(iv) Plastic zone radius (i.e. locus and maximum extent of plastic zone);
(v) Charts of SZW, plastic zone radius r_y and ratio of SZW/r_y for various plastic loading conditions; and
(vi) Shear-lip sizes for the 3-D analyses.

Table 2.1: Dimensions of Specimens

Dimensions	Specimen	
	DT-350WT-08	DT-350WT-02
Beam Length, L (mm)	181	181
Beam Span, S (mm)	164	164
Crack Length, a (mm)	14*	14*
Beam Width, W (mm)	41	41
Beam Thickness, B (mm)	8	2

*a = 12 mm plus 0.254 mm pressing followed by fatigue extension to 14 mm

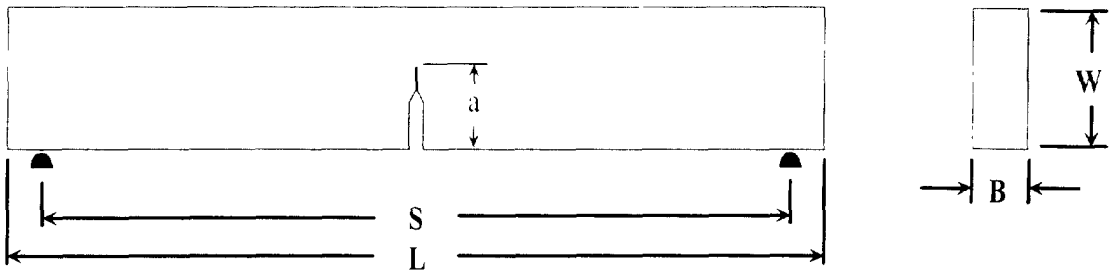

Figure 2.1: Configuration of DT Specimen

3. FINITE ELEMENT MODEL

3.1 Finite Element Approach

The ABAQUS finite element software [3] was used to model the elastic-plastic behaviour of the DT specimen. The software has a wide range of non-linear materials models and can account for large strains and displacements. However, the HyperMesh [4] general-purpose pre- and post-processing program was used for model generation and results processing. Details of the finite element models are provided below.

3.2 Finite Element Meshes

The HyperMesh code was used to generate the finite element models of the DT and non-standard specimens, which were then translated to ABAQUS input files. Figure 3.1 shows the finite element mesh that was used in the Phase II study for the DT-350WT-08 specimen. This mesh, which contained first order plain-strain elements (4 node quadrilateral and 3 node triangular elements) was used as the control. This mesh is designated as Mesh 1L. Note that in order to reduce the problem size only one-half of the structure was modelled using symmetry conditions. Additional mesh configurations were also considered to investigate influence of mesh configuration on the plastic zone development. The first mesh considered was a second order version of the control mesh and is designated as Mesh 1Q. This mesh consisted of quadratic plain-strain elements instead of the linear elements used in Mesh 1L. The next two additional finite element meshes, designated as Mesh 2L and Mesh 3L, are shown in Figures 3.2 and 3.3, respectively. The mesh in Figure 3.2 involves more refinement in the crack tip area and the mesh in Figure 3.3 involves a coarser element configuration around the crack tip. The final mesh considered was the second order version of the Mesh 3L (Figure 3.3), and is designated as Mesh 3Q. The second order version of Mesh 2L was not considered because the results of Meshes 1L and 1Q were very close, indicating that beyond this level of refinement the extra computer costs involved by the use of quadratic element is not justified by the improvement in solution accuracy. For clarity, the mesh designations and their descriptions are summarized in Table 3.1.

The 3-D meshes used for the DT-350WT-08 and DT-350WT-02 specimens were obtained by extruding the Mesh 3L model in the thickness direction. The Typical 3-D mesh is shown in Figure 3.4.

3.3 Material Models

An incremental rate independent plasticity theory available in the ABAQUS finite element program [3] was used for the material constitutive model. This standard model for plasticity is summarized in the Phase I report [1]. Figure 3.5 shows the stress-strain behaviour of 350 WT steel material. Details are provided in [2].

3.4 Boundary Conditions and Loading

The following boundary conditions were applied:

At the support: $v = 0$

Along the center line: u=0;

where, u, v are the displacements components in the longitudinal and transverse directions.

The load was applied in the form of a displacement of the top midpoint of the beam specimen. The displacement was applied incrementally in steps of about 0.0001 mm (see ref. [2])

Table 3.1: Summary of Finite Element Meshes

Mesh Designations	Description
Mesh 1L	Mesh used in Phase II, with linear plain strain elements
Mesh 1Q	Mesh used in Phase II, but with quadratic plain strain elements
Mesh 2L	More refined mesh, with linear plain strain elements
Mesh 3L	Coarser mesh, with linear plain strain elements
Mesh 3Q	Coarser mesh, with quadratic plain strain elements

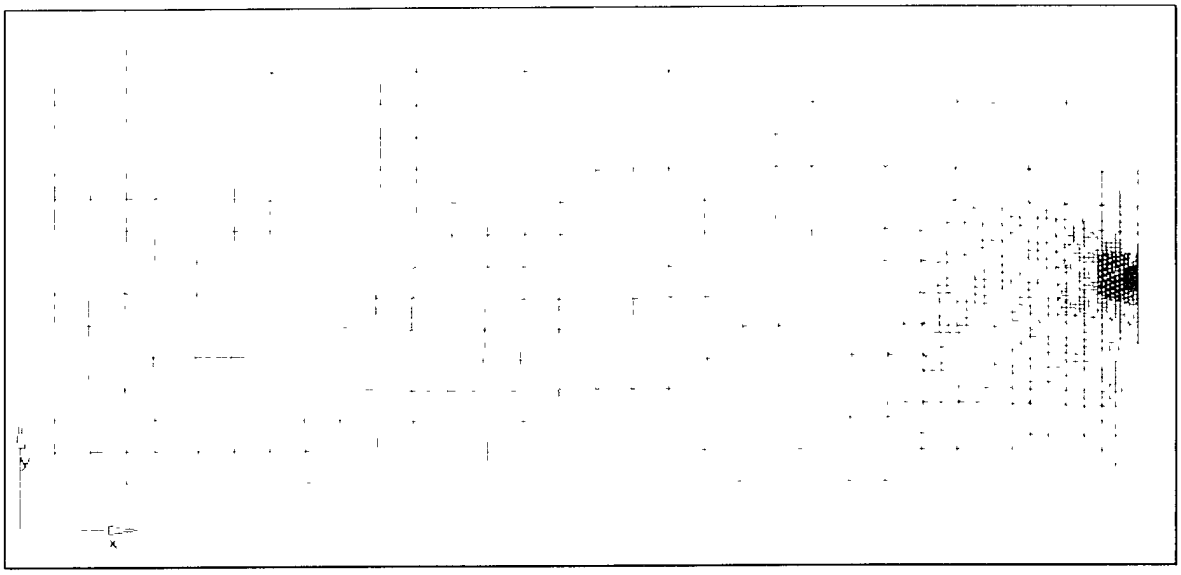

(a)

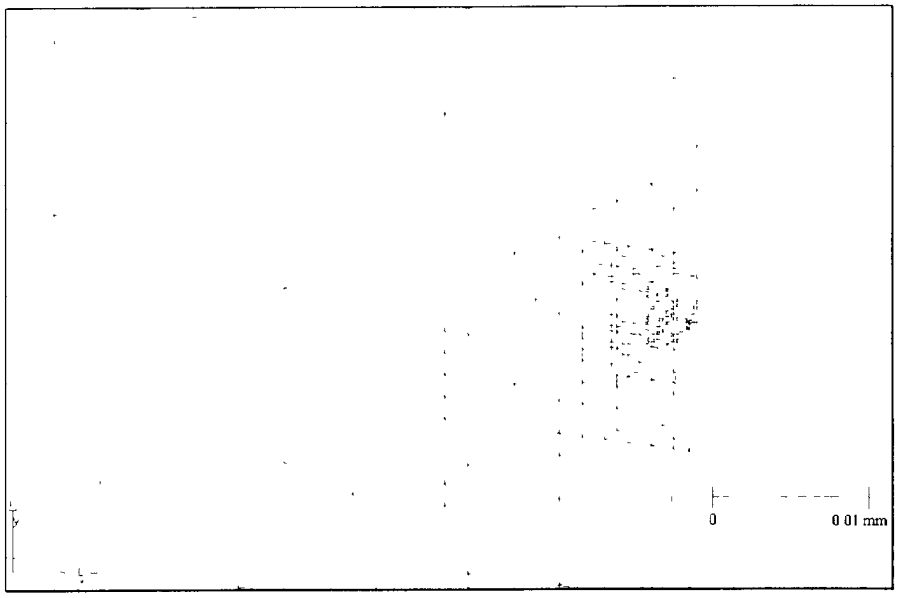

(b)

Figure 3.1: FE Mesh of 8.0 mm Thick DT Specimen (Mesh 1L): (a) Full Mesh (b) Close-up Mesh

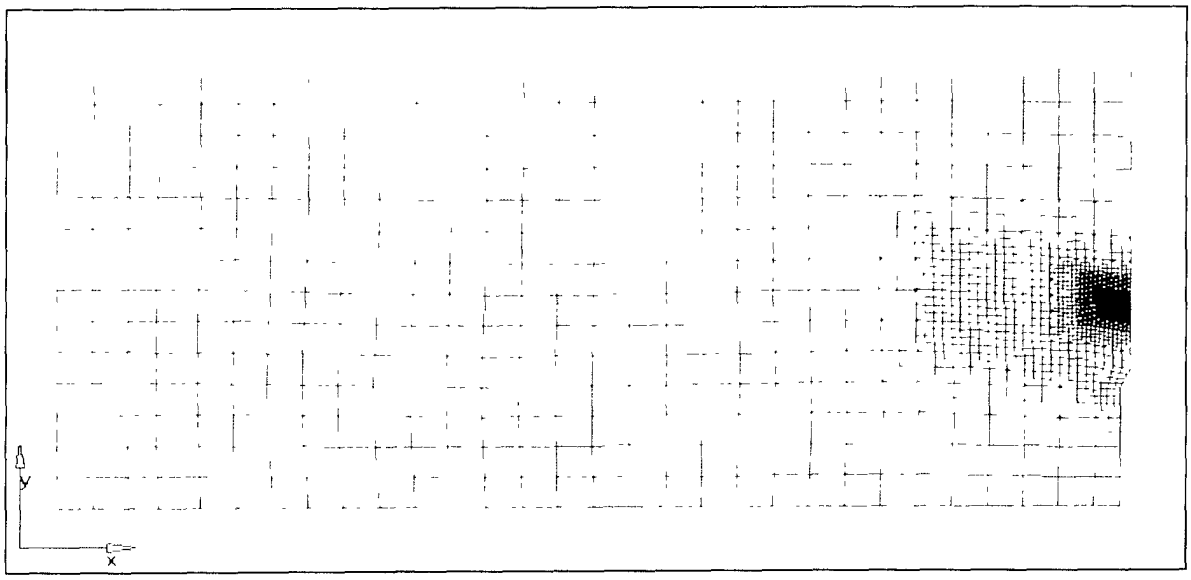

(a)

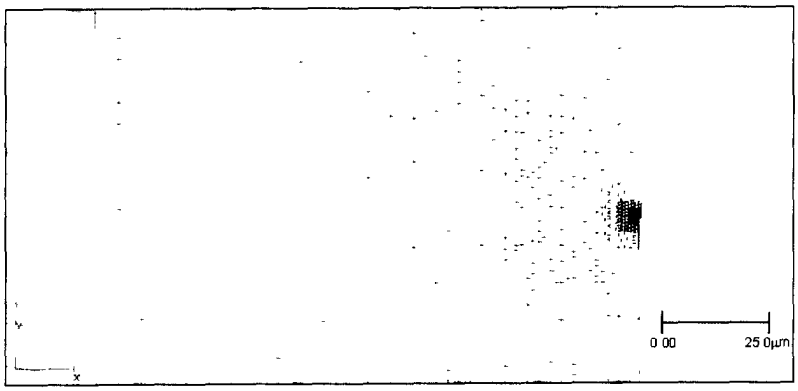

(b)

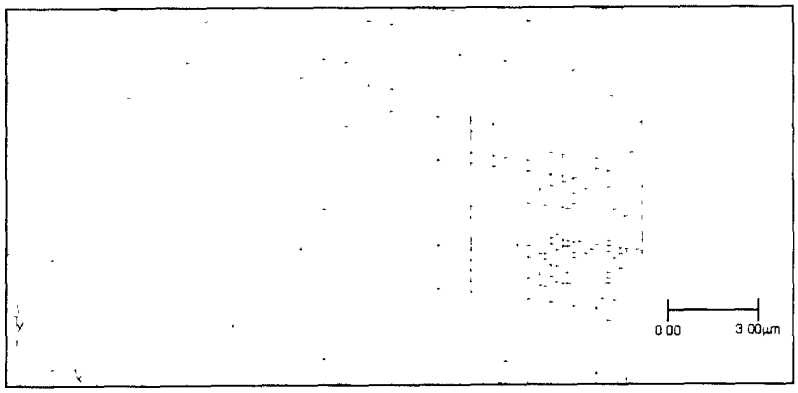

(c)

Figure 3.2: Refined FE Mesh of 8.0mm Thick DT Specimen (Mesh 2L)

3.6

(a)

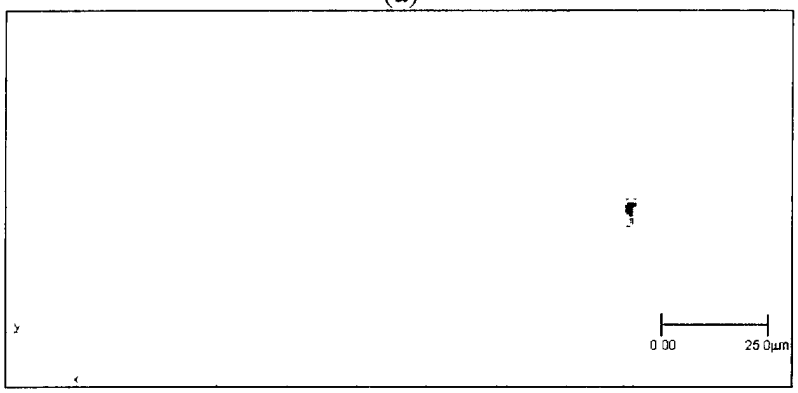

(b)

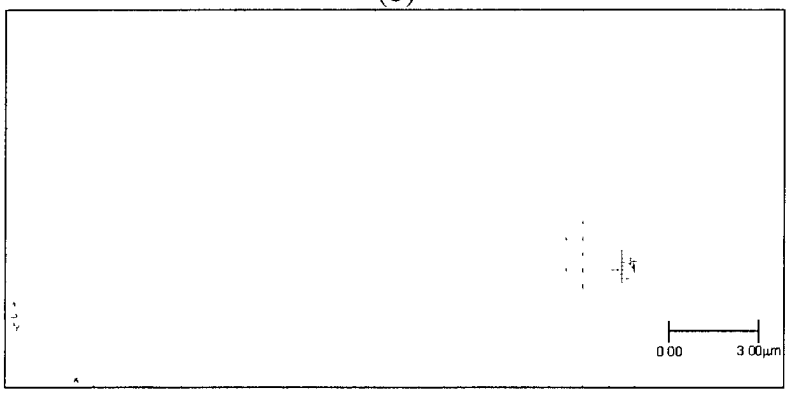

(c)

Figure 3.3: Coarser FE Mesh of 8.0mm Thick DT Specimen (Mesh 3L)

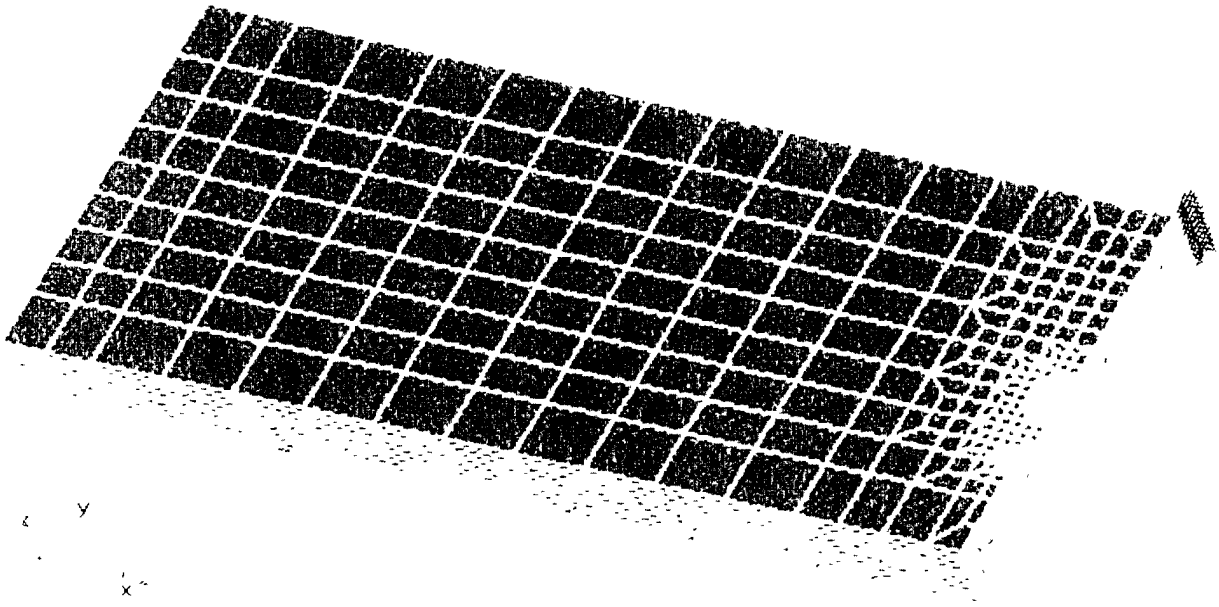

Figure 3.4: 3-D Mesh of 8 mm Thick Standard Specimen

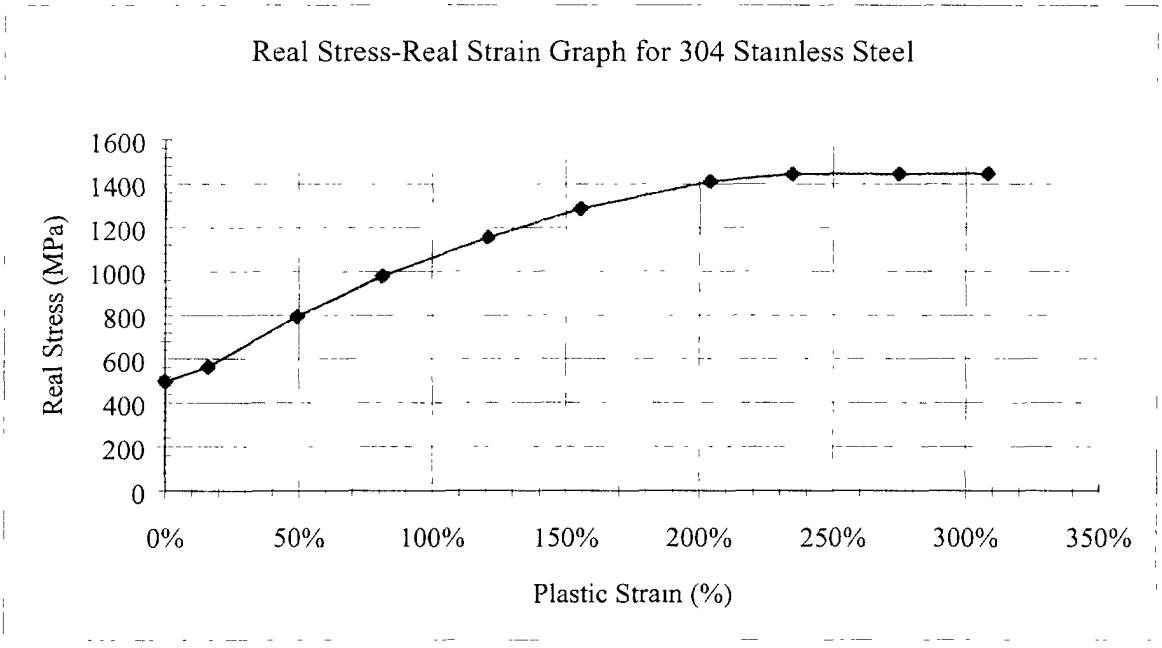

Figure 3.5: Stress–Strain Curve of 350WT Steel

4. RESULTS AND DISCUSSIONS

This chapter discusses the results of the study. For each specimen, results of the deformation profiles, plastic zone development, plastic strain, plastic radius, and stretch zone width are provided in the following section.

4.1 Deformation Profiles

Figures 4.1, 4.2 and 4.3 show the displacement contours of the DT-350WT-08 specimen at the last displacement increment, for Meshes 1L, 2L and 3L, respectively. This displacement contour pattern was observed at all displacement increments for all the specimens. Detailed deformed and undeformed plots near the crack tip of the DT-350WT-08 specimen are also shown in the figures illustrating the very large stretching (strain) of the elements near the crack tip. It is seen that for the meshes considered the deformation profiles are not significantly affected by the mesh configurations.

4.2 Plastic Zone Development

The development of the plastic zone around the crack tip was determined using contour plots of the equivalent plastic strain or von Mises stress at various steps of the loaded specimen. As was noted in the previous studies [1,2], the shapes and sizes of the plastic zones using the von Mises stress or equivalent stress are very similar. Thus for brevity only the strain contours are presented in this section. The von Mises stress contours for the new finite element models are presented in the Appendix. Also, the plastic strain and von Mises stress contours for the Mesh 1L model, which are referred to in the discussions, are not presented here, as they have already been presented in reference [2].

Figures 4.4 to 4.7 show the plastic strain contours at various displacement levels in the DT-350WT-08 specimens, using the Mesh 1Q, 2L, 3L and 3Q models, respectively. Note that different scales are used to plot the contours at different load levels due to the differences in the magnitudes of the strains at the various levels. However, it is seen that for a given model the sizes

of the plastic zone as well as the magnitude of the maximum plastic strains increase with the applied displacement. It is also seen that the shape of the plastic strain contours for all the models are similar. Smooth contours are observed for the 1Q (original mesh with quadratic elements),and 2L (more refined mesh with linear elements) models. Moreover, the observed contours are very similar to the ones obtained for the original (Mesh 1L) model. Given that the 1Q and 2L models required considerably larger amounts of computer resources, it can be concluded that the Mesh 1L model is a reasonably good model for evaluating the plastic zone development. The plastic strain contours obtained from the 3L and 3Q meshes are somewhat rough, indicating that these meshes may not be optimum for assessing the plastic zone development. However, they do provide reasonable predictions of the plastic zone sizes.

4.3 Plastic Strain Behaviour

Figure 4.8 summarizes the plastic strain behaviour of all five finite element models. In the figure the maximum strains in the specimen attained are plotted against the non-dimensionized displacements (D_L/B). It is seen that for all models the plastic strain increases parabolically with the D_L/B ratio. At low D_L/B ratios (less than 0.03) all models predict the same plastic strain profiles. Differences in the predictions occur at higher D_L/B ratios, but are still close. The Mesh 1L and 2L models provided results up to D_L/B ratio of 0.07, beyond which point the analysis could not continue. However, models 1Q, 3L and 3Q provided results up to D_L/B ratios of about 0.1, and exhibit very sharp gradients beyond $D_L/B = 0.07$.

4.4 Plastic Zone Radius (r_y), Stretch Zone Width (SZW) and ry/SZW Ratio

The plastic zone radius, ry, and the stretch zone width (SZW) at various load levels were measured from the plastic zone configurations. The plastic zone is taken as the distance from the crack tip to the farthest point of the plastic zone. The stretch zone width (SZW) is given by the distance from the crack tip to the interface of the plastic zone with the side of the crack. These are illustrated schematically in Figure 4.9. Figure 4.10 shows the variation of the plastic radius with DL/B, for all the five models. The plastic zone radius increases with the non-dimensionized midpoint displacement, similar to the plastic strain behaviour. The predictions from all five models are close, indicating that all the mesh configurations considered are suitable for predicting

the plastic zone size.

Figure 4.14 shows the variation of the stretch zone width (SZW) at various displacement levels. The SZW increases parabolically with D_L/B ratio and all models except Mesh 3L provide very similar responses. The Mesh 3L results are erratic due to difficulties in measuring the relatively small SZW sizes from the coarse finite elements. This mesh is therefore not suitable for computing the SZW sizes.

The ratios of the plastic zone radius to stretch zone width (r_y/SZW) were also computed and presented in Figure 4.12. All curves tend to increase steadily and exhibit distinct points where the slopes of the curves change significantly. It would seem that the first portion of the curves represent elastic fracture whereas the second portion represents elastic plastic fractures. At any given D_L/B ratio, the r_y/SZW values provided by Meshes 1Q and 2L are larger than that provided by the original Phase II mesh (ie Mesh 1L), whereas the r_y/SZW values provided by Meshes 3L and 3Q are smaller. It turns out that the results from Mesh 3L are significantly lower than the results of all other models, making Mesh 3L unsuitable for determination of the r_y/SZW ratio.

The following additional observations can be made regarding the behaviour of the r_y/SZW:

(i) the slope of the first portion of the curve is always larger than that of the second portion;

(ii) the r_y/SZW for all models (except Mesh 3L) in the elastic-plastic region is in the range of 70 – 140.

4.5 3-D Analyses

Three-dimensional analyses were performed for the 8mm and 2mm thick specimens using the mesh configuration shown in Figure 3.4. As shown in Figure 3.4, the mesh has ten solid elements through the specimen thickness. However, due to the very small in-plane dimensions of the elements (see 2-D models) the aspect ratios of these elements are very poor. The 2mm thick specimen was used to investigate the influence of the poor element aspect ratio on the results. By

maintaining the same number of elements (10) across the thickness the thickness of the 2mm specimen a four-fold improvement of the aspect ratios of the elements around the crack tip was achieved. No significant difference was observed in the general pattern of the results obtained from the two specimen configurations, suggesting that the poor aspect ratio did not significantly affect the general trend of the results for the 8mm thick specimen. Obviously, one way of improving the element aspect ratios will be to increase the number of elements through the thickness, but the computer time and storage requirements were so large that it was prohibitive to refine the model further.

The displacement profiles and plastic zone development with incremental load was similar to the 2-D cases. Of interest here is the through-thickness plasticity. Figures 4.14 and 4.15 show the plastic strain development in the 2mm and 8mm thick specimens, respectively. As noted above, the pattern of the plastic strains from the two cases are very similar. From the morphology of fracture surface the shear lip can be obtained as shown schematically in Figure 4.13(a), where the shear lip size, s, is obtained as the distance from the yield surface to the original surface at the specimen edge. As the load is increased, the plastic strain contour shapes tend towards the shape depicted by the fracture surface in Figure 4.13(a). However, at the last increment considered in the study, the predicted fracture morphology is of the shape shown in Figure 4.13(b), which is somewhat different from the one shown in Figure 4.13(a). As a result, it is difficult to measure the shear lip at a point. Using the plastic strain profile in Figure 4.15(a) and considering the point at which the plastic curves are closest (Location A) the shear lip size for the 8 mm thick specimen is estimated to be s = 2.4 mm, for a shear index of 0.6. However, further investigations are necessary to provide a more accurate measure the shear lip size. Such an additional effort, which might include the application of a failure criterion and refinement of the mesh in the thickness direction, could not be carried out in the present study because of limited resources.

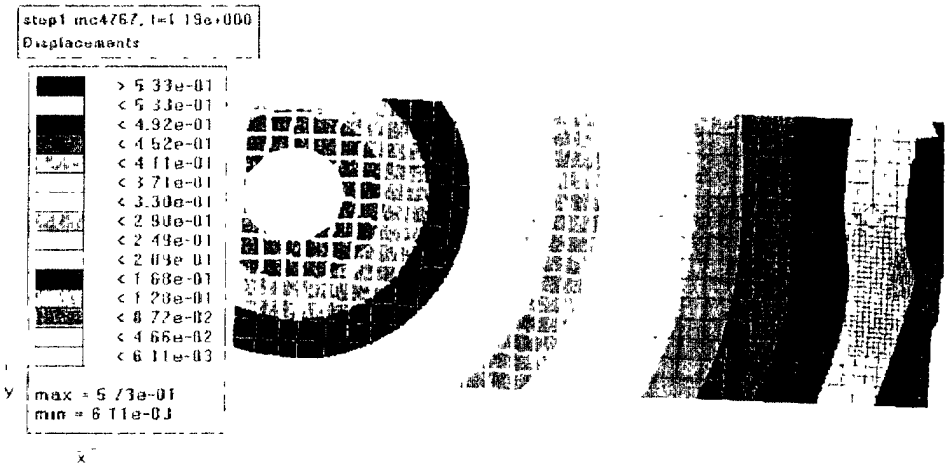

(a)

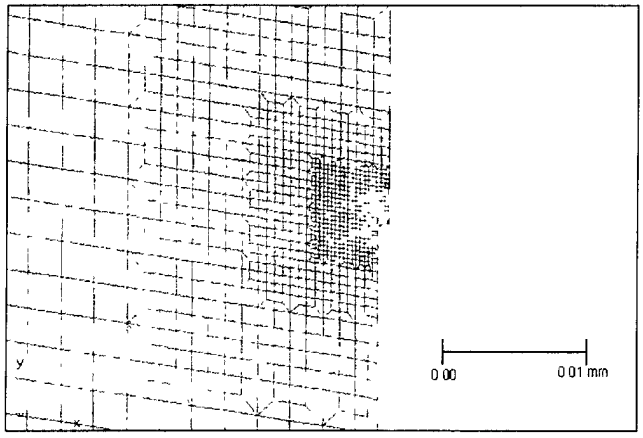

(b)

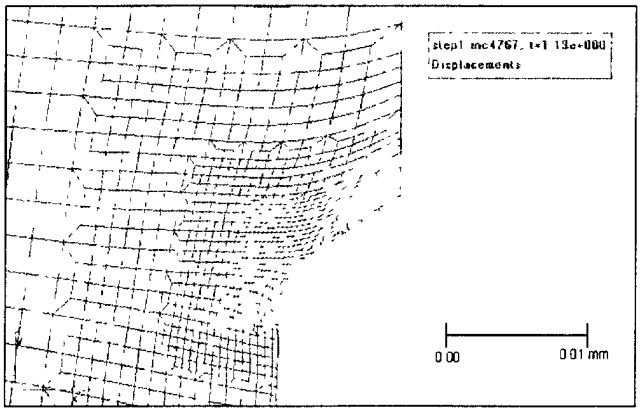

(c)

Figure 4.1: Final Displacements of Phase I Model of DT-350WT-08 Specimen:
(a) Displacement Contours; (b) Undeformed Shape Near Crack Tip; (c) Deformed Shape Near Crack Tip

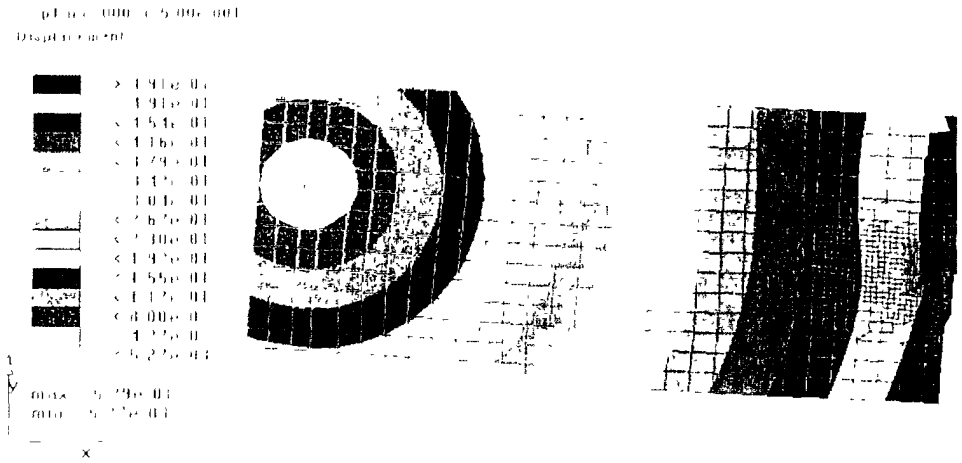

(a)

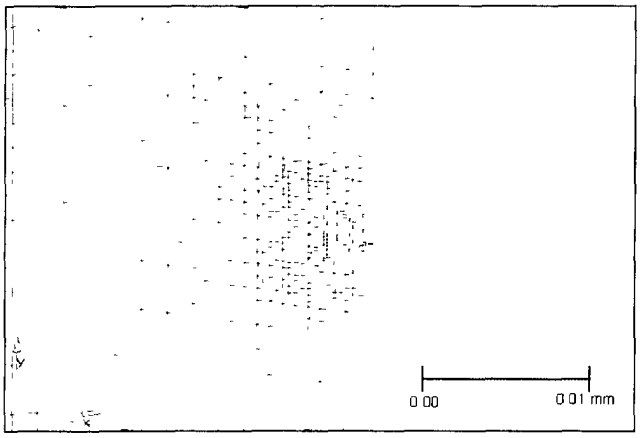

(b)

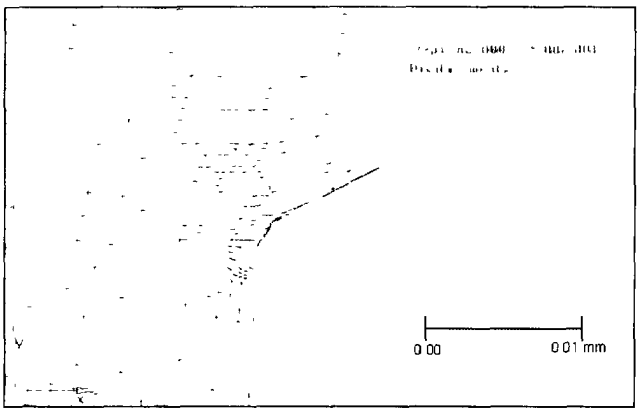

(c)

Figure 4.2: Final Displacements of Refined Model of DT-350WT-08 Specimen: (a) Displacement Contours; (b) Undeformed Shape Near Crack Tip; (c) Deformed Shape Near Crack Tip

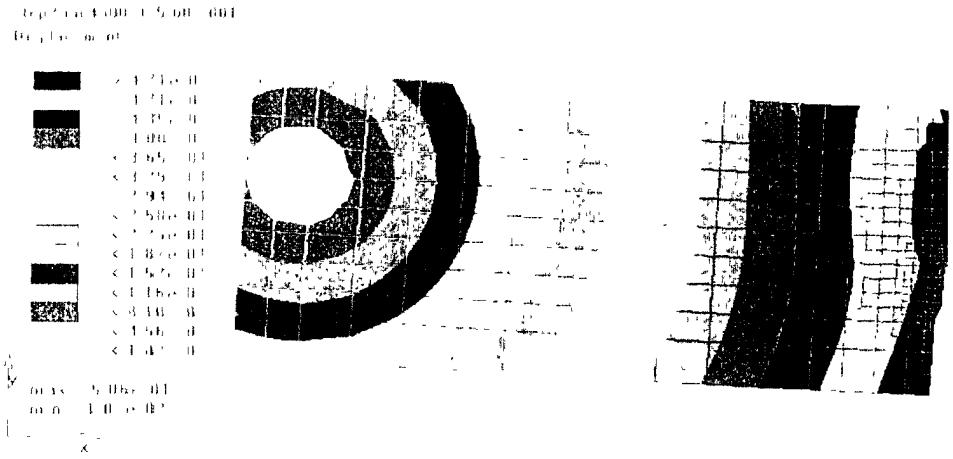

(a)

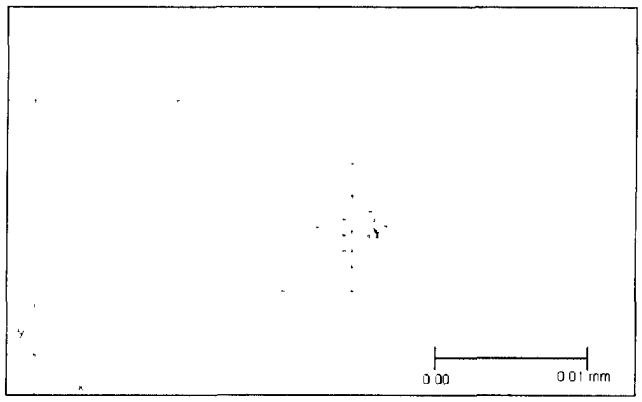

(b)

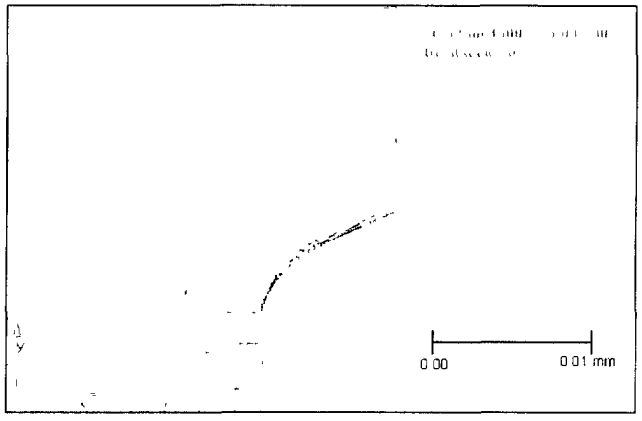

(c)

Figure 4.3: Final Displacements of Coarser Model of DT-350WT-08 Specimen: (a) Displacement Contours; (b) Undeformed Shape Near Crack Tip; (c) Deformed Shape Near Crack Tip

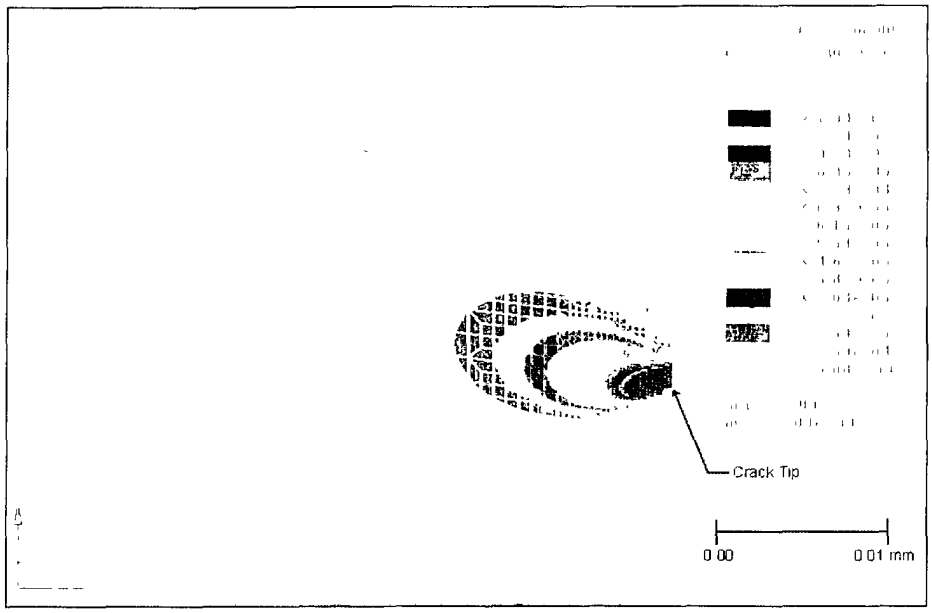

(a)

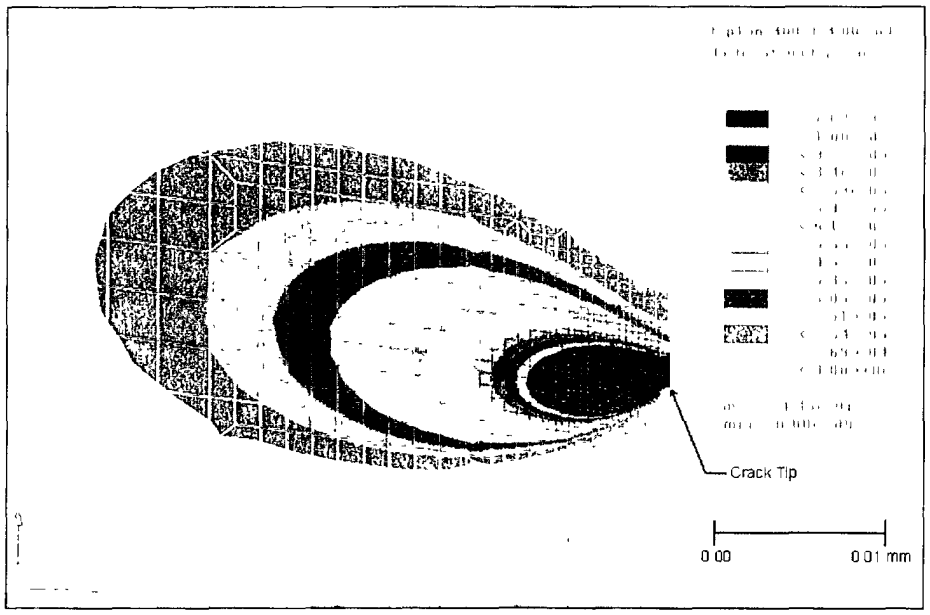

(b)

Figure 4.4: Plastic Strain Contours in DT-350WT-08 Specimen Using Mesh 1Q
(a) $D_L / B = 0.00339$ (b) $D_L / B = 0.00542$

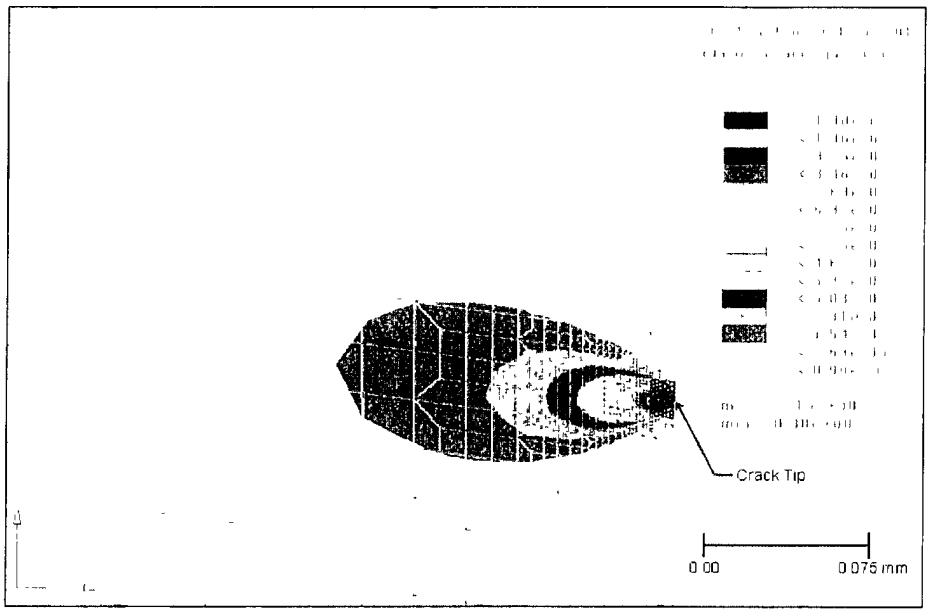

(c)

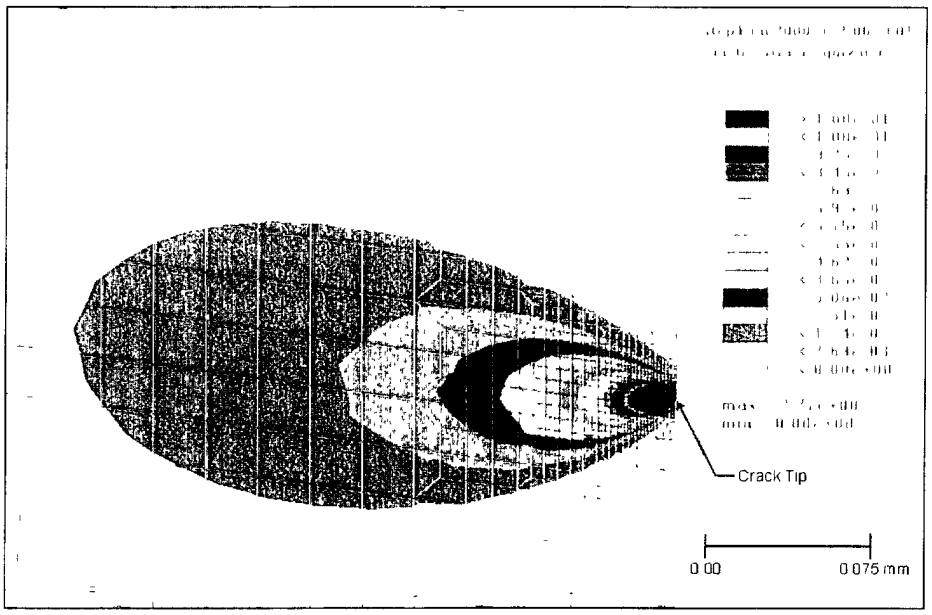

(d)

Figure 4.4: Plastic Strain Contours in DT-350WT-08 Specimen Using Mesh 1Q
(c) $D_L / B = 0.02037$ (d) $D_L / B = 0.02718$

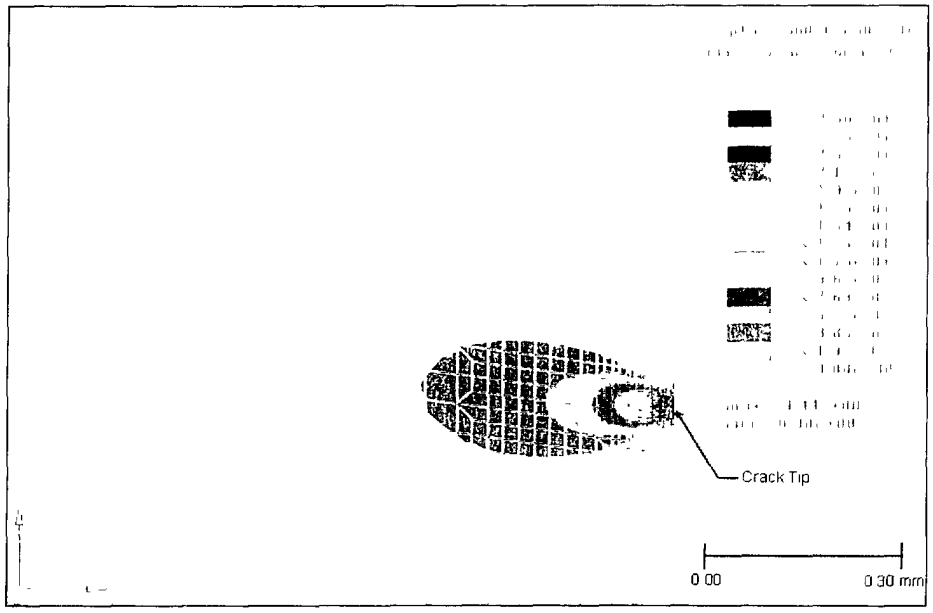

(e)

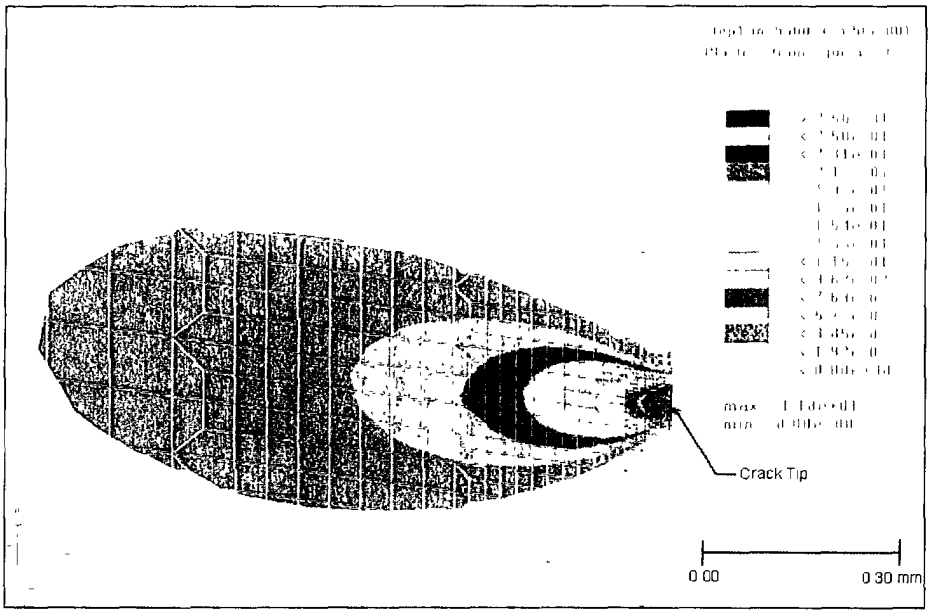

(f)

Figure 4.4: Plastic Strain Contours in DT-350WT-08 Specimen Using Mesh 1Q
(e) $D_L / B = 0.04805$ (f) $D_L / B = 0.07728$

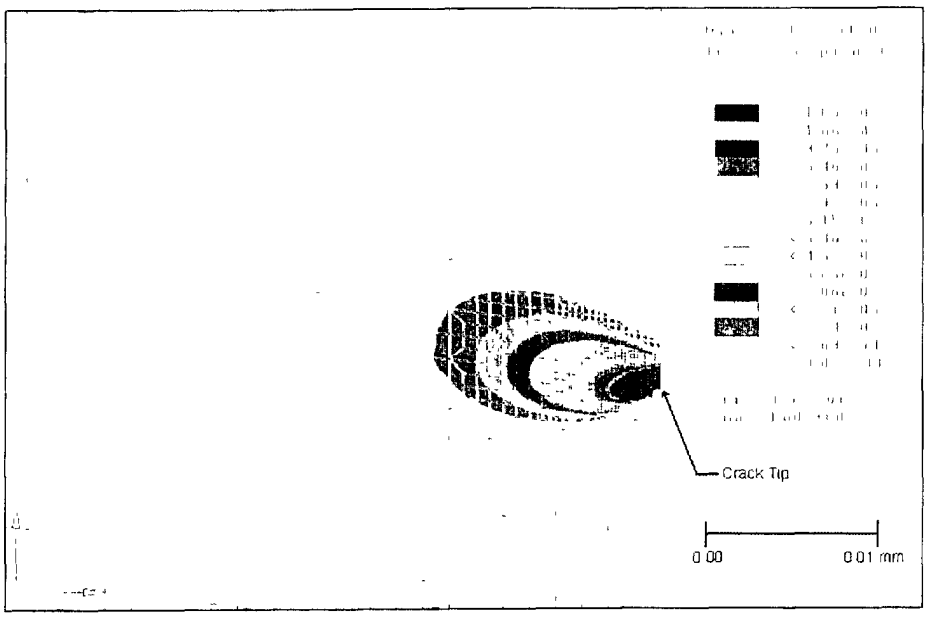

(a)

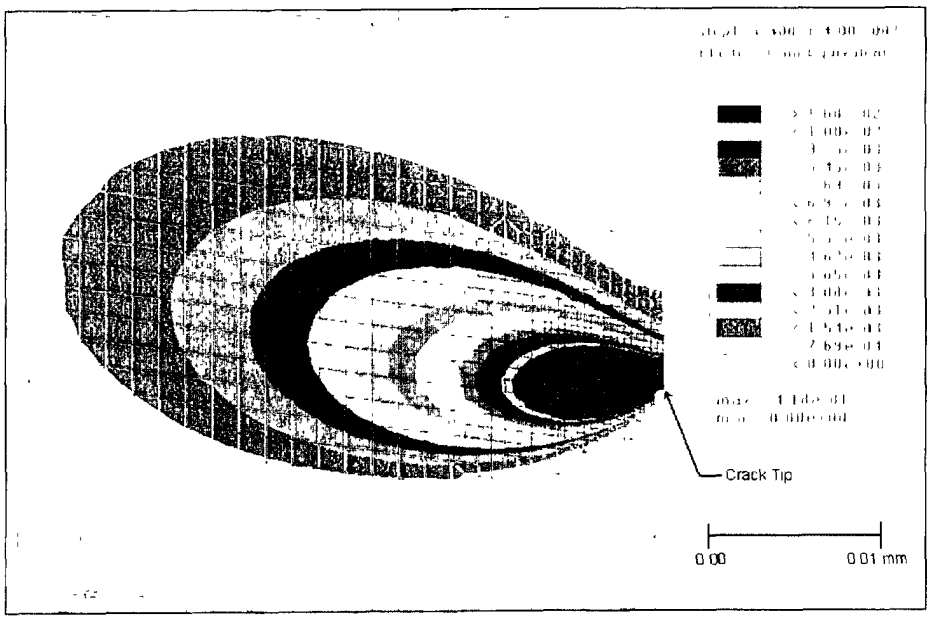

(b)

Figure 4.5: Plastic Strain Contours in DT-350WT-08 Specimen Using Mesh 2L
(a) $D_L / B = 0.00340$ (b) $D_L / B = 0.00543$

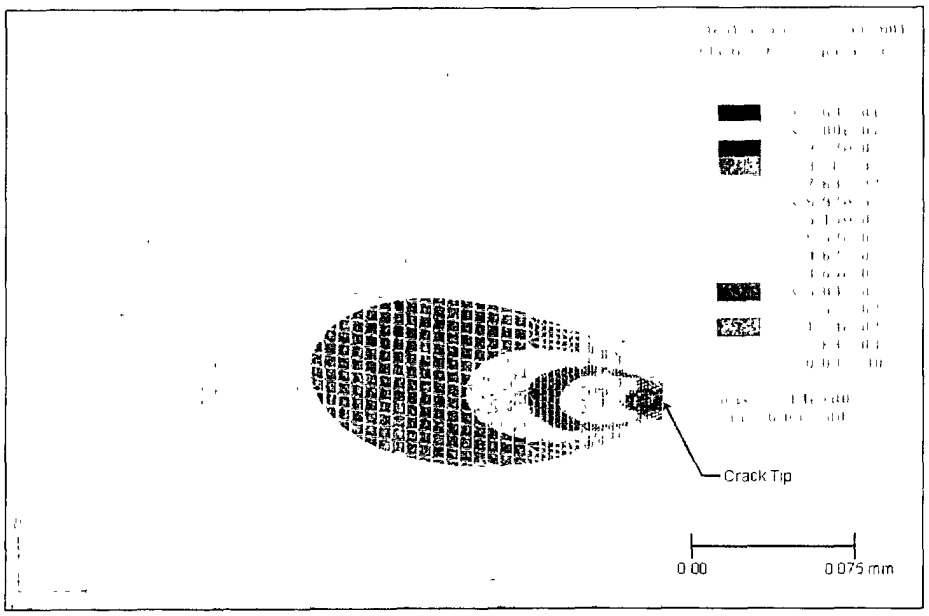

(c)

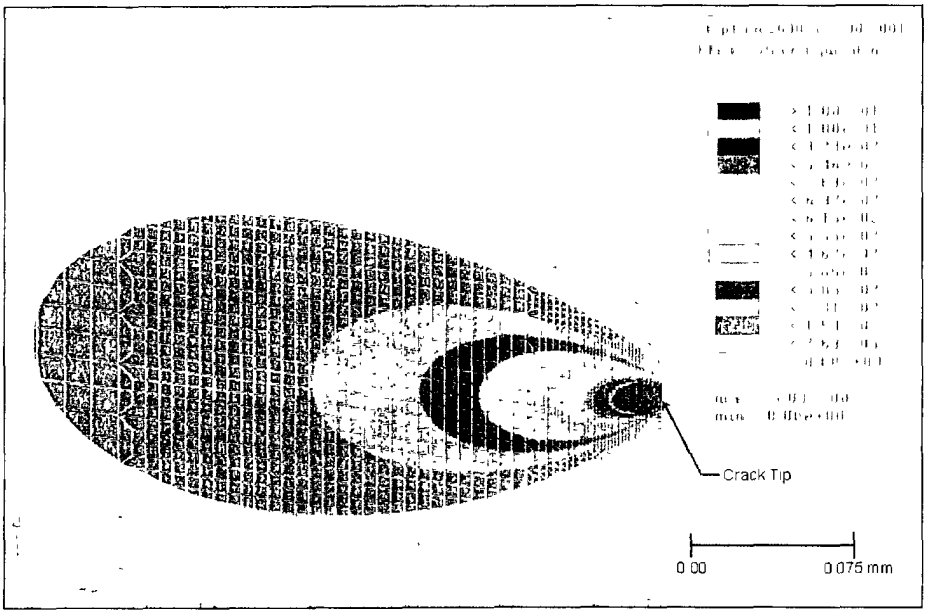

(d)

Figure 4.5: Plastic Strain Contours in DT-350WT-08 Specimen Using Mesh 2L
(c) $D_L / B = 0.02038$ (d) $D_L / B = 0.02720$

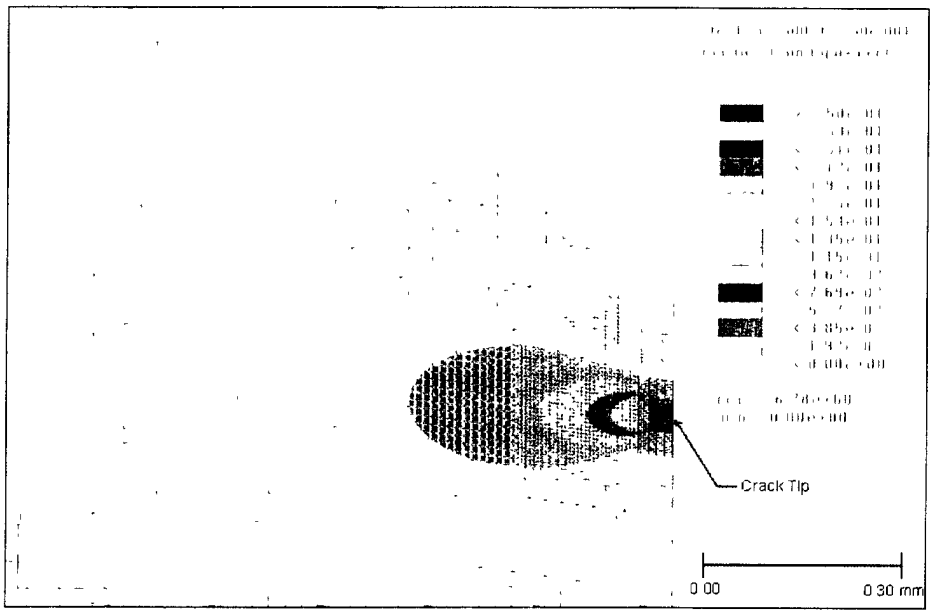

(e)

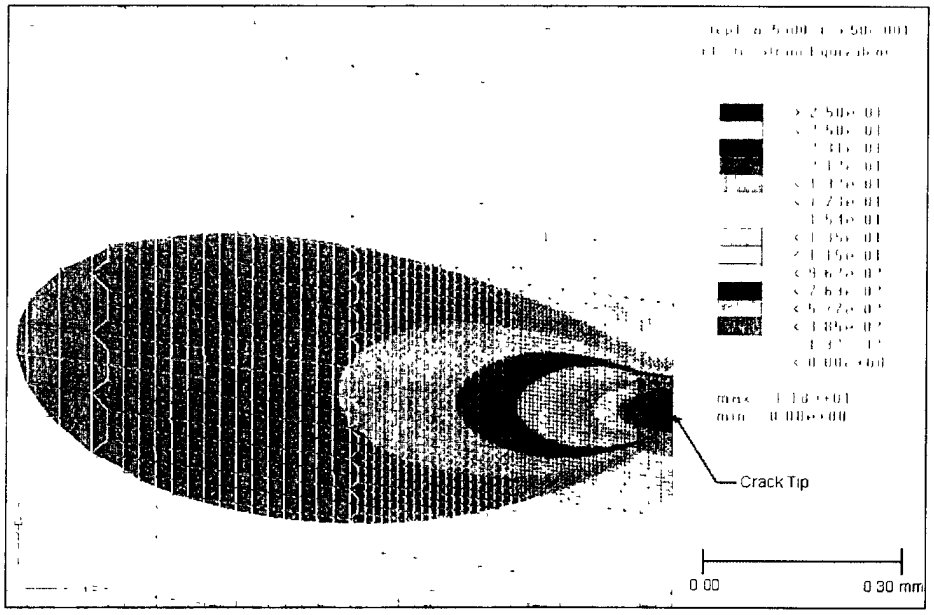

(f)

Figure 4.5: Plastic Strain Contours in DT-350WT-08 Specimen Using Mesh 2L
(e) $D_L / B = 0.04788$ (f) $D_L / B = 0.07677$

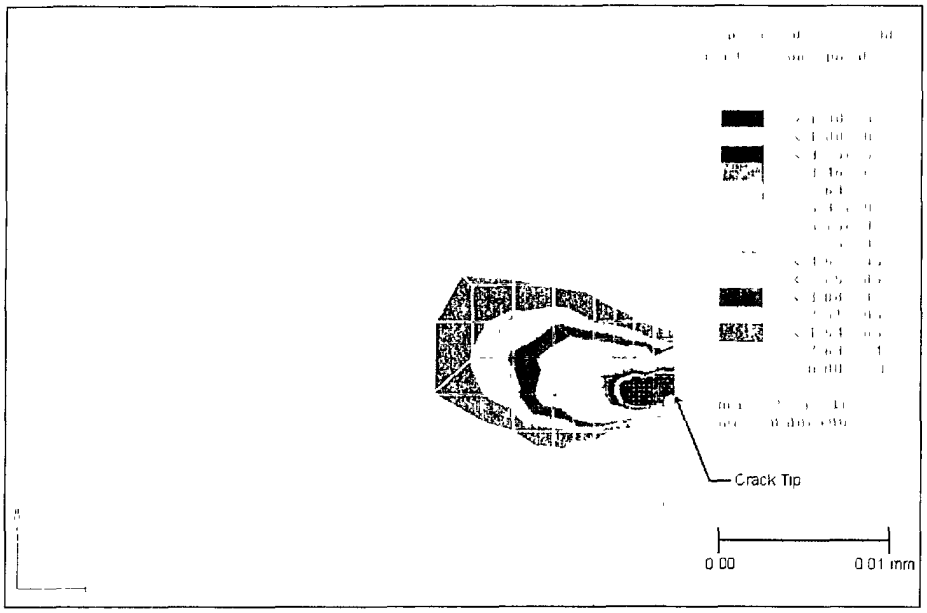

(a)

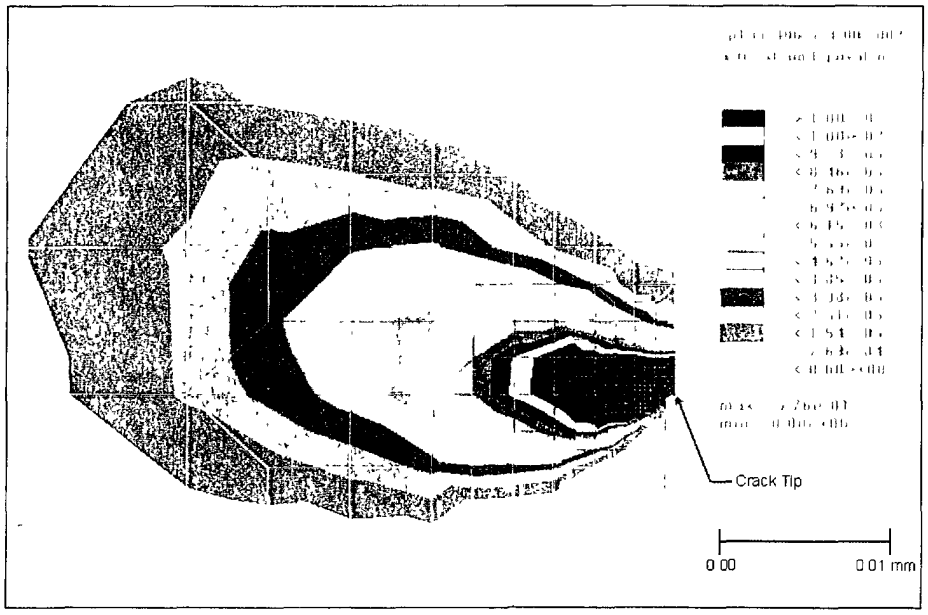

(b)

Figure 4.6: Plastic Strain Contours in DT-350WT-08 Specimen Using Mesh 3L
(a) $D_L / B = 0.00341$ (b) $D_L / B = 0.00546$

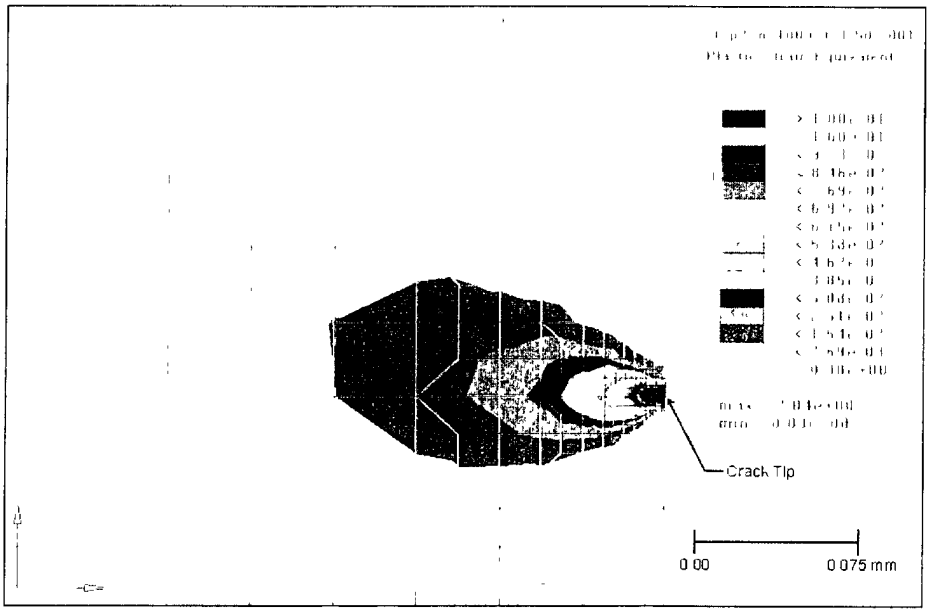

(c)

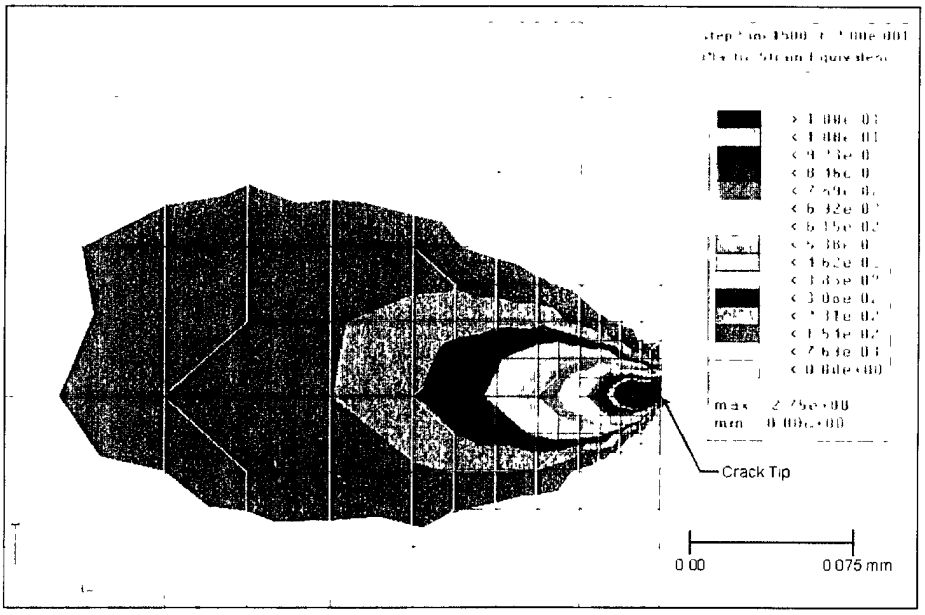

(d)

Figure 4.6: Plastic Strain Contours in DT-350WT-08 Specimen Using Mesh 3L
(c) $D_L / B = 0.01981$ (d) $D_L / B = 0.02634$

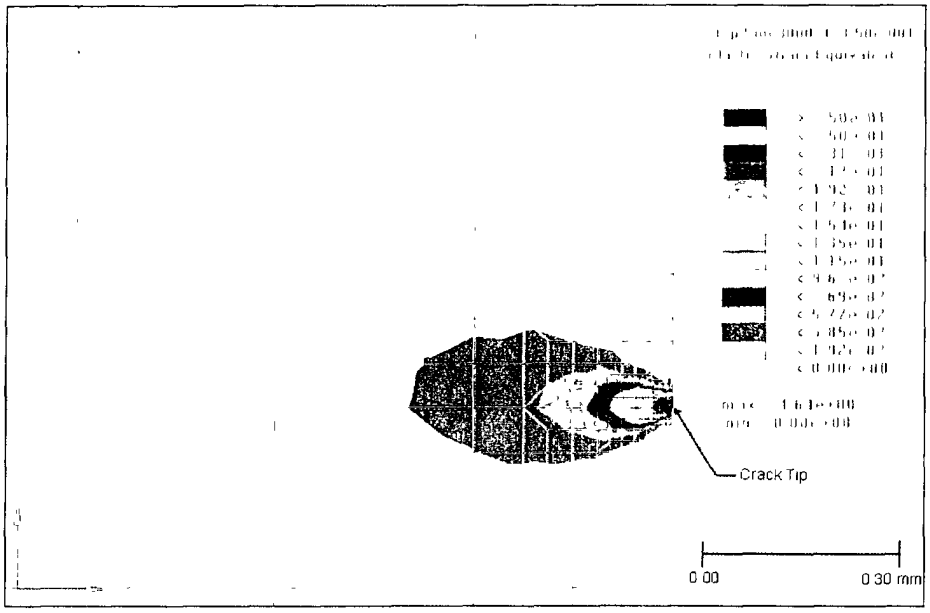

(e)

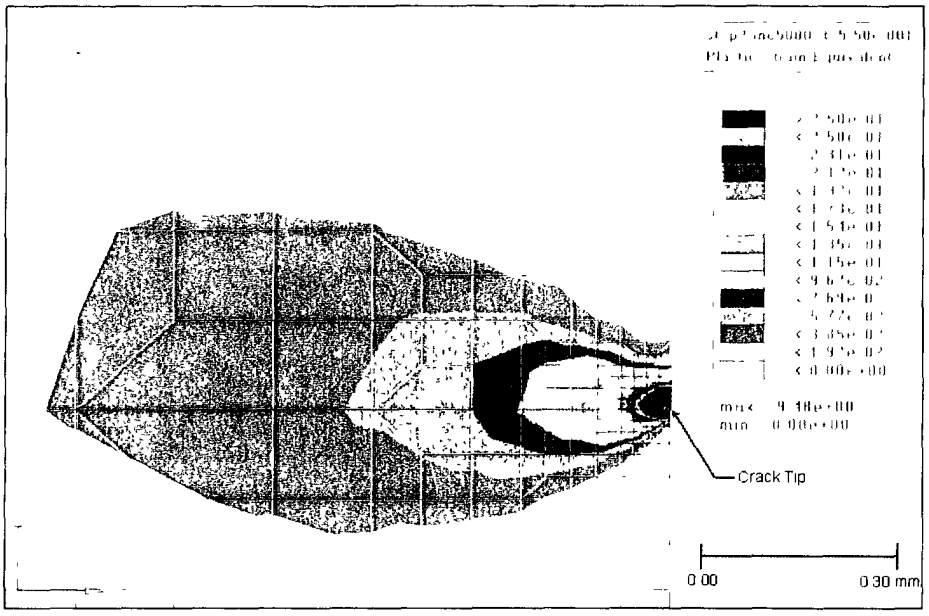

(f)

Figure 4.6: Plastic Strain Contours in DT-350WT-08 Specimen Using Mesh 3L
(e) D_L / B = 0.04499 (f) D_L / B = 0.06912

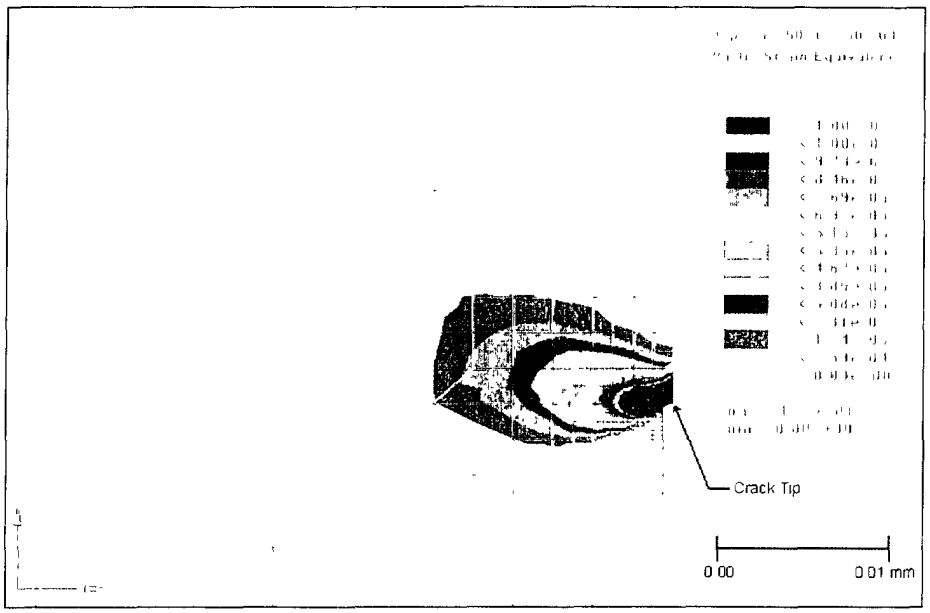

(a)

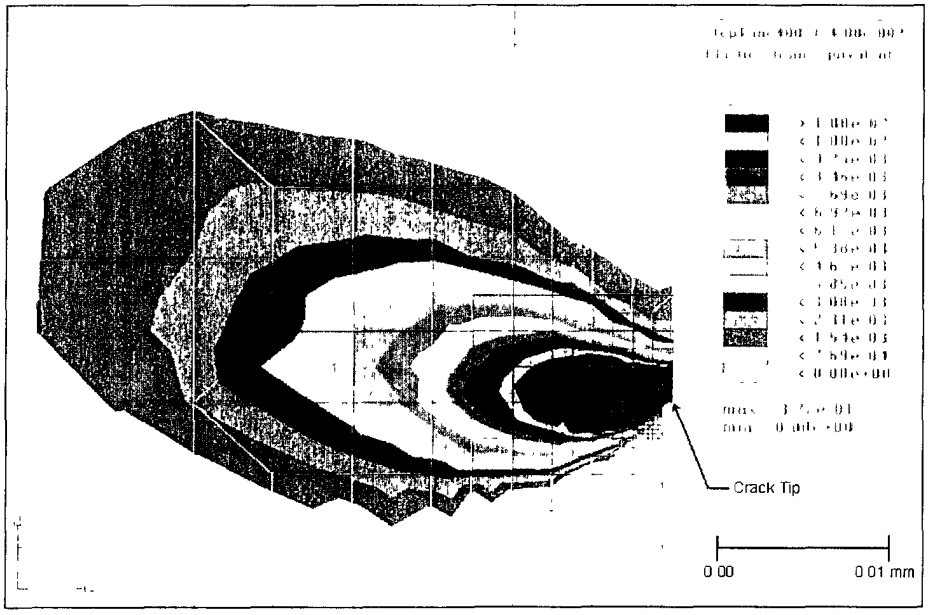

(b)

Figure 4.7: Plastic Strain Contours in DT-350WT-08 Specimen Using Mesh 3Q
(a) $D_L / B = 0.00340$ (b) $D_L / B = 0.00544$

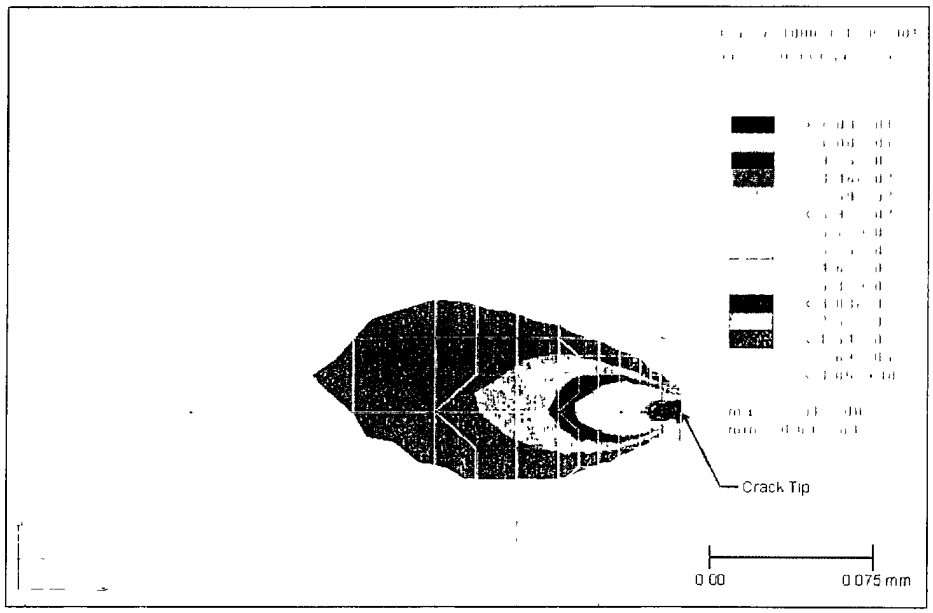

(c)

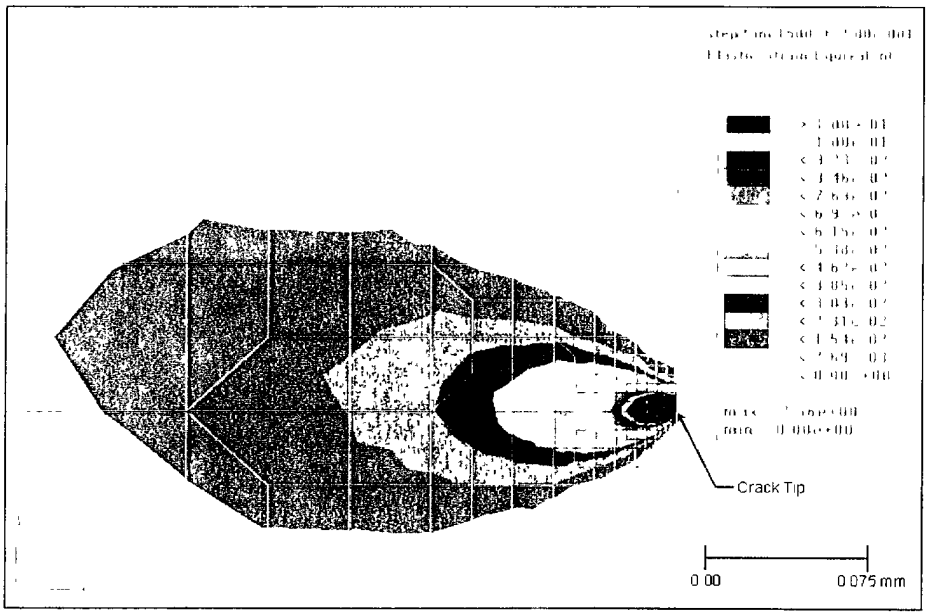

(d)

Figure 4.7: Plastic Strain Contours in DT-350WT-08 Specimen Using Mesh 3Q
(c) $D_L / B = 0.01942$ (d) $D_L / B = 0.02580$

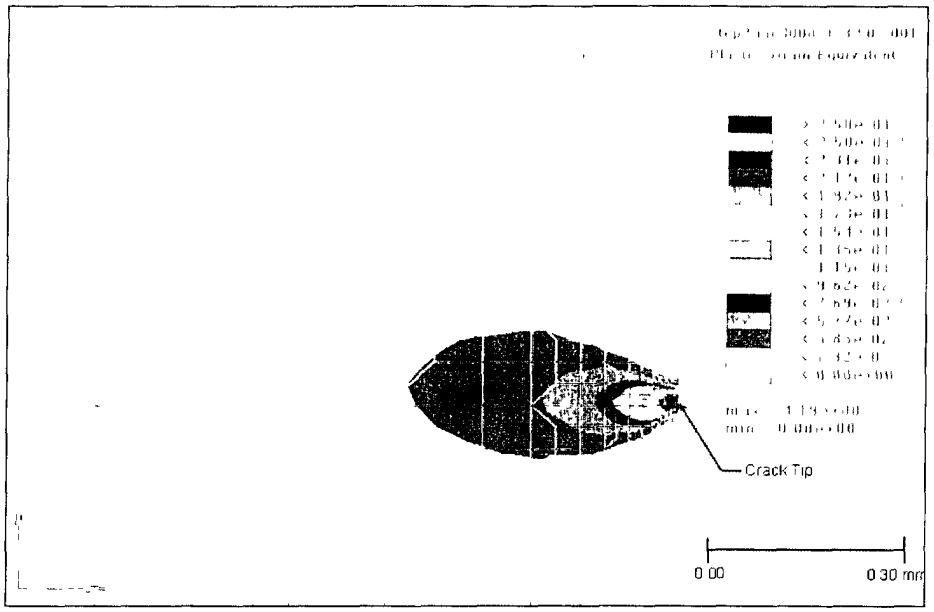

(e)

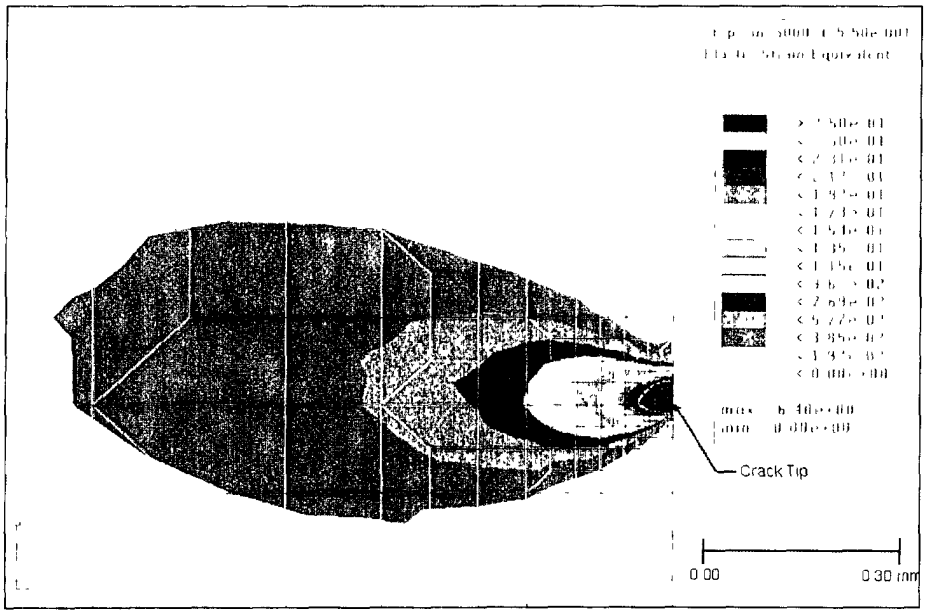

(f)

Figure 4.7: Plastic Strain Contours in DT-350WT-08 Specimen Using Mesh 3Q
(e) $D_L / B = 0.04513$ (f) $D_L / B = 0.07058$

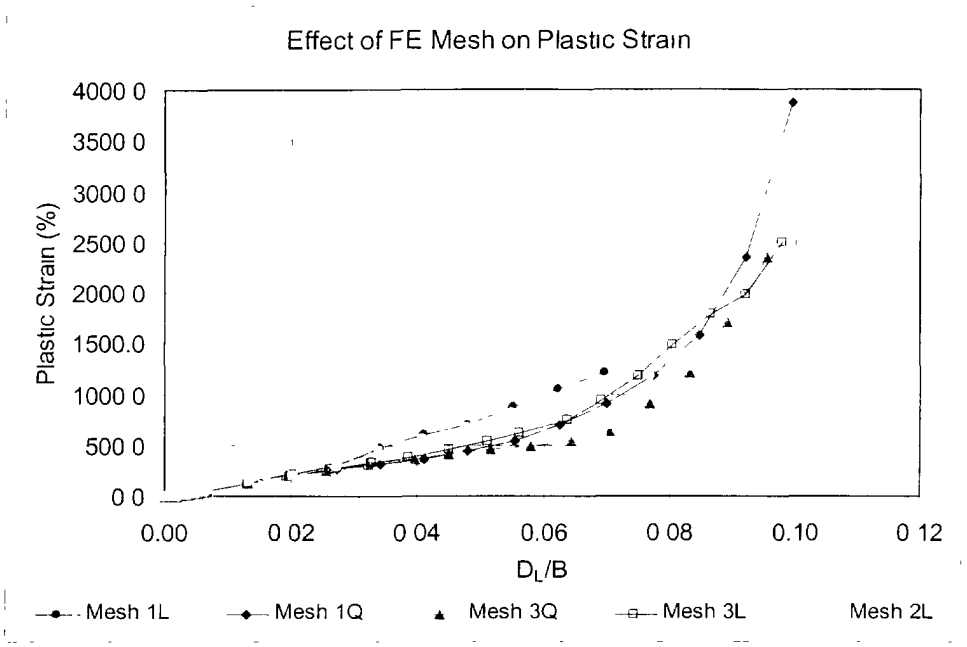

Figure 4.8: Variation of Maximum Plastic Strain with Non-Dimensionalized Displacement for all Specimens

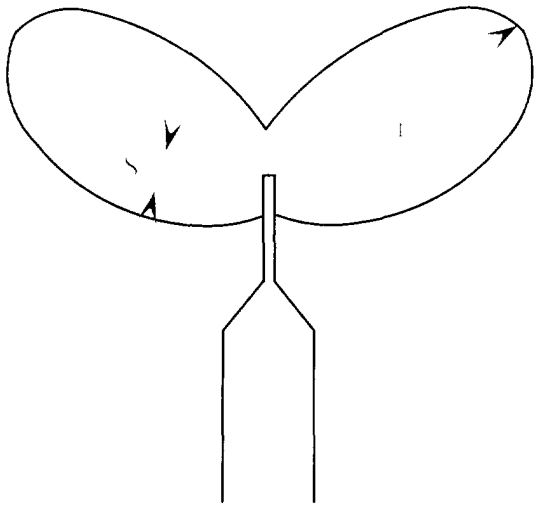

Figure 4.9: Schematic Illustration of Plastic Radius (r_y) and Stretch Zone Width (SZW)

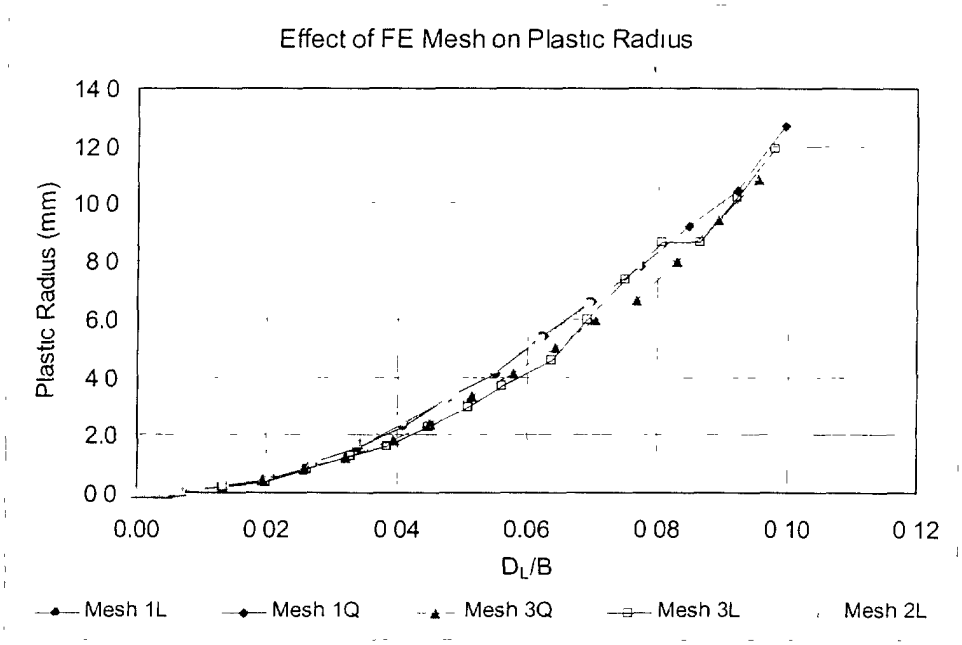

Figure 4.10: Variation of Plastic Radius with Non-Dimensionalized Displacement for all Specimens

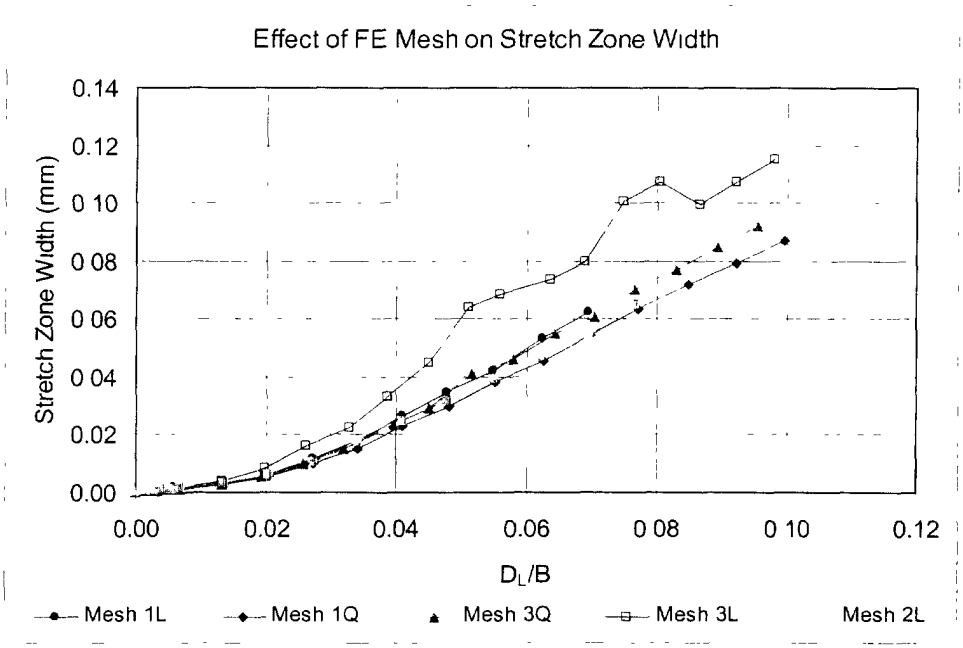

Figure 4.11: Variation of SZW with Non-Dimensionalized Displacement for all Specimens

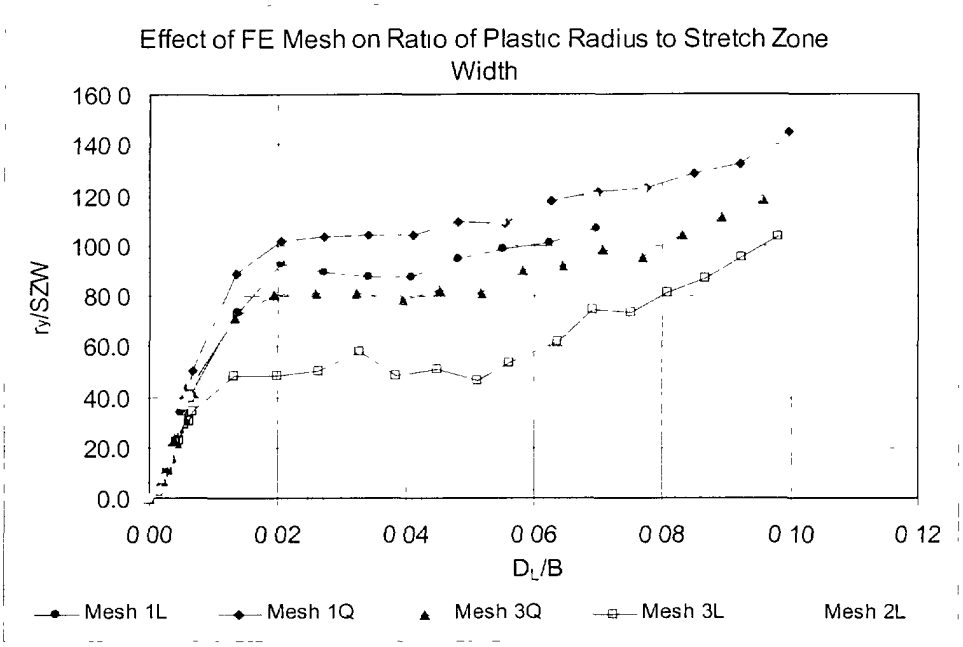

Figure 4.12: Variation of r_y/SZW with Non-Dimensionalized Displacement for all Specimens

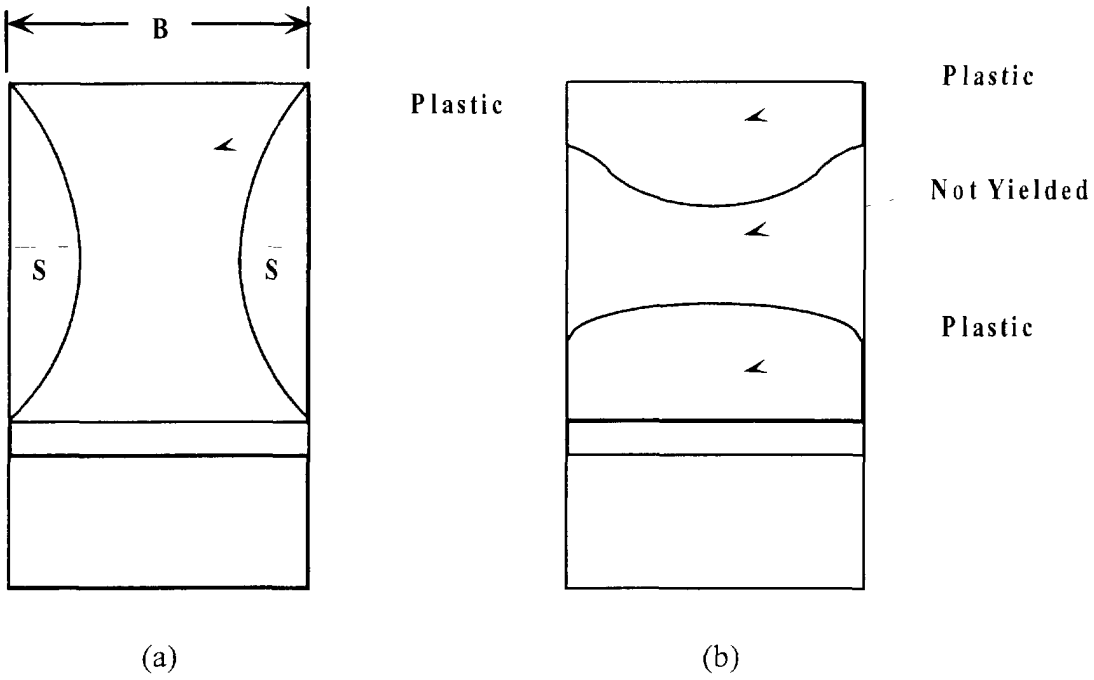

Figure 4.13 - Schematic Illustration of Progression of Shear Lip
(a) Experimental (b) Numerical (FEM)

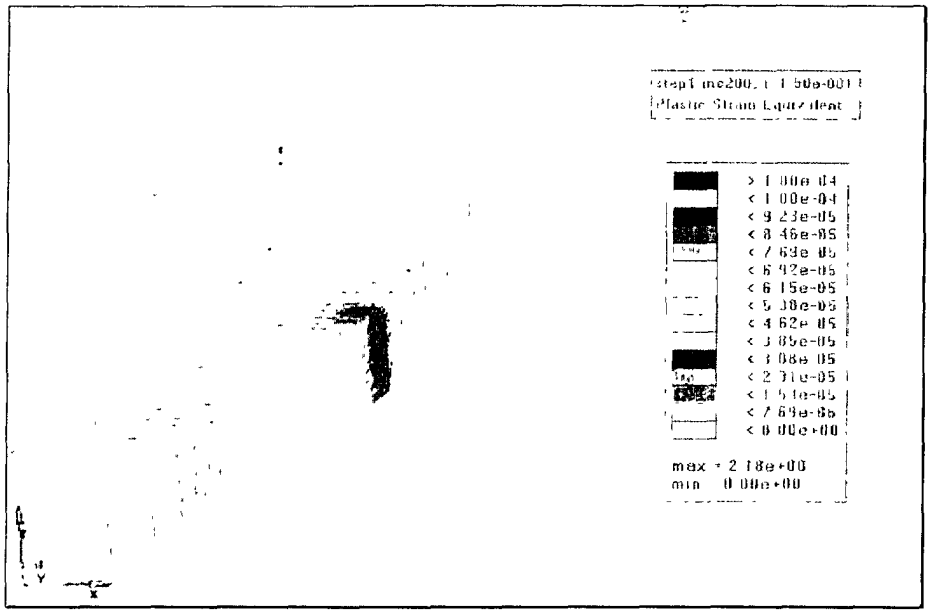

(a)

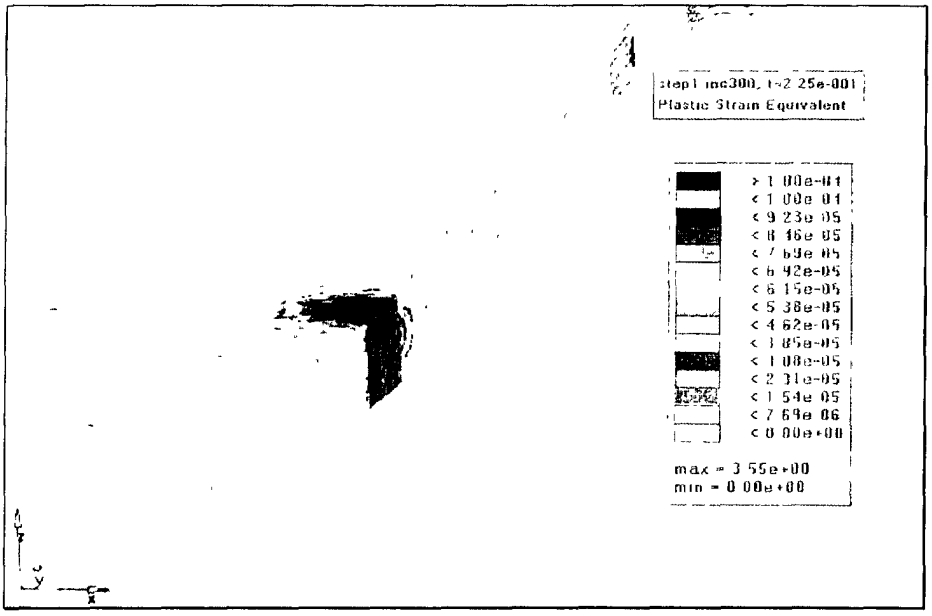

(b)

Figure 4.14 - Plastic Strain Contours of 3-D Model of 2mm Thick Coupon (a) D_L / B = 0.082 (b) D_L / B = 0.123

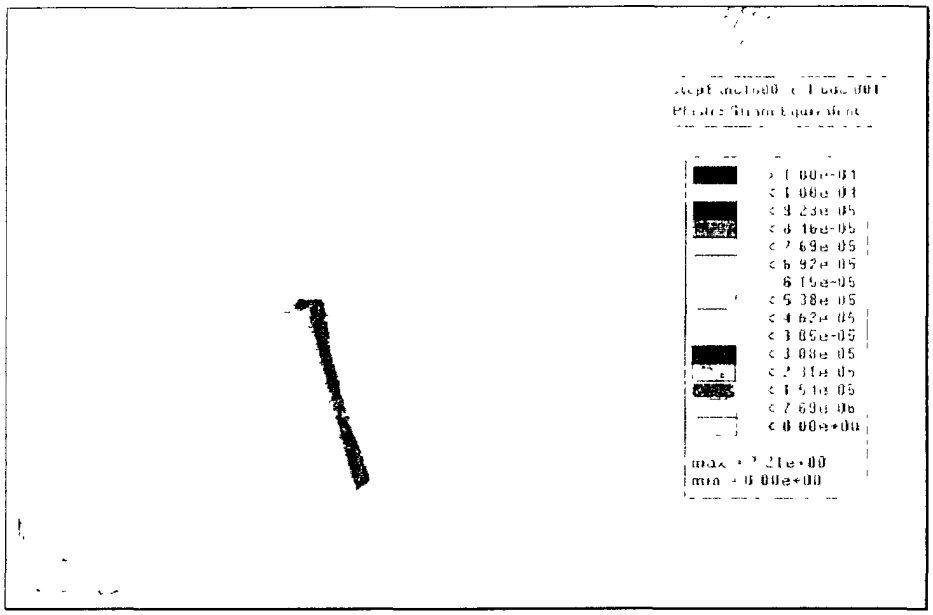

(a)

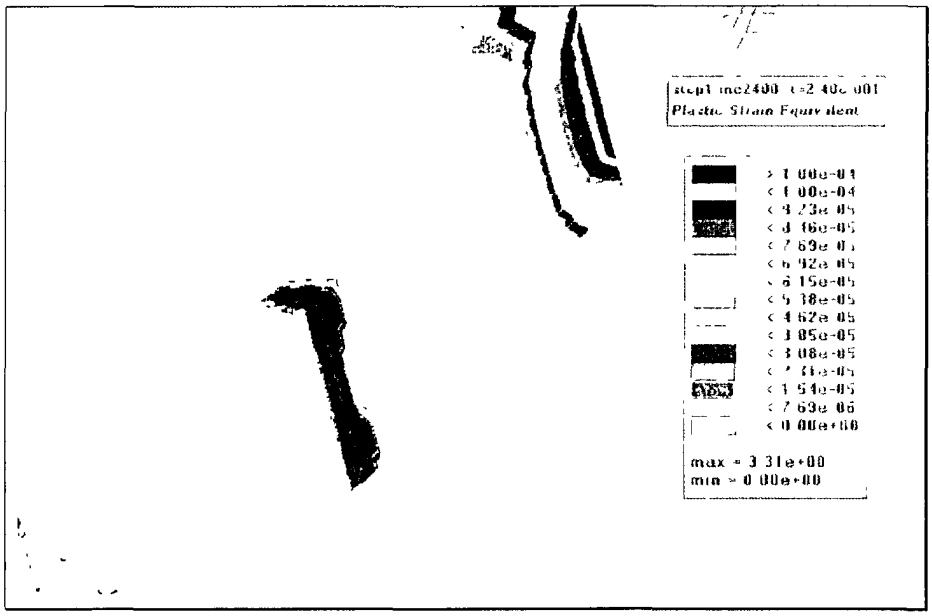

(b)

Figure 4.15 - Plastic Strain Contours of 3-D Model of 8mm Thick Coupon (a) D_L / B = 0.022, (b) D_L / B = 0.033 and (c) D_L / B = 0.095

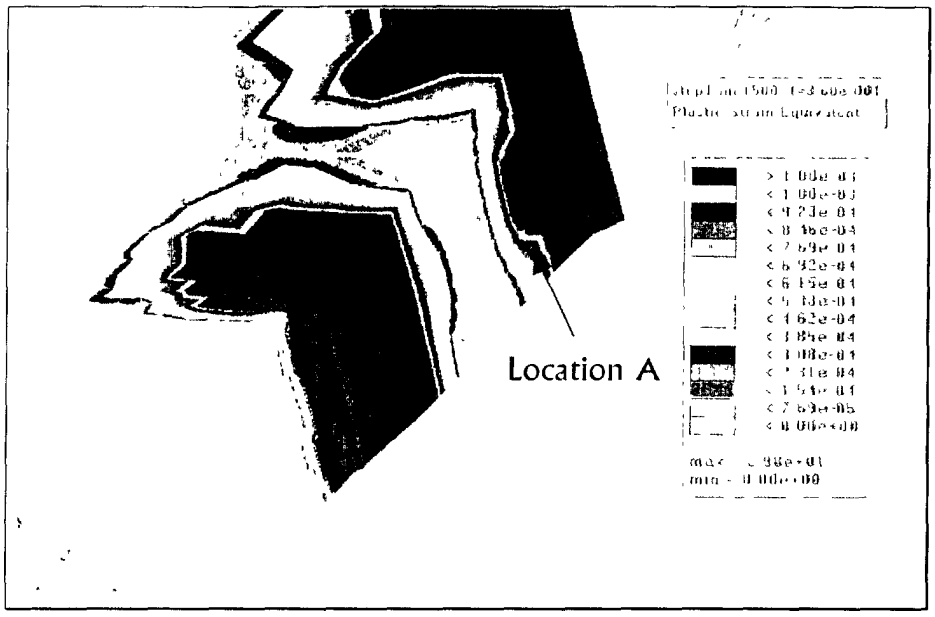

(c)

Figure 4.15 - Plastic Strain Contours of 3-D Model of 8mm Thick Coupon (a) D_L / B = 0.095, (b) D_L / B = 0.095 and (c) D_L / B = 0.095

5. SUMMARY, CONCLUSIONS AND RECOMMENDATIONS

5.1 Summary and Conclusions

This study is a continuation of efforts to investigate plastic zone development in three-point bend fracture specimen to provide an understanding of crack tip blunting (stretch zone) to plastic zone size (radius), in order to be able to predict the upper limit where elastic plastic fracture becomes invalid. Finite element analyses of an 8mm specimen made of 350WT steel were performed. The scope of the present study included investigations of the effects of various modeling (mesh) parameters on the behaviour of 2-D finite element models; and 3-D modeling to investigate shear lip behaviour. The ABAQUS finite element code was used to perform incremental elastic-plastic analysis of the specimens.

The results computed included the progression of plastic strain, plastic radius (r_y), stretch zone width (SZW), and the r_y/SZW ratio with plastic displacement. Contour plots of plastic strain and von Mises stresses are presented at selected plastic displacement levels. It was found that the plastic radius and maximum plastic strains were not too sensitive to the mesh size around the crack tip, whereas the SZW is highly sensitive to mesh size around the crack tip. Thus the r_y/SZW ratio also depends on mesh configuration. In creating meshes around the tip, it is necessary to ensure that the sizes of the elements around the tip are such that several elements are contained in the region from the crack tip to the side of the crack where the yield line intersects the side of the crack.

In general, the meshes with quadratically interpolated elements (Meshes 1Q and 3Q) provided smoother plastic strain contours than their corresponding meshes with linearly interpolated elements (Meshes 1L and 3L), and hence enabled more accurate measurements of the plastic zone sizes. The same trend is observed with mesh refinement. However, the use of higher order elements or mesh refinement required significantly larger amounts of computer time, computer storage and cost. Therefore, for practical purposes, a compromise mesh configuration, such as mesh 1L, has to be used to provide acceptable accuracy at a reasonable cost.

The 3-D analyses confirmed the in-plane plastic zone patterns obtained from the 2-D analyses. The 3-D analyses also provided some insight on the shear lip behaviour. However, the results obtained from the analyses did not provide a distinct point at which to measure the shear lip. At a plastic displacement of 0.0975B (B = specimen thickness) the shear index was estimated to be 0.6 at the point where the yield lines were closest. Further studies are required to provide more accurate estimates of the shear lip size.

5.2 Recommendations

It is recommended that further studies on the 3-D behaviour be performed to provide better insight into the shear lip sizes for various specimen configurations (eg. 8mm, 16mm and 25mm thick specimens). Such a study could be corroborated by experimental and analytical studies discussed by Matthews (1996). It is also recommended that the results of all phases of the study be compared to the experimental results when they are available. Based on these comparisons, it might be necessary to refine the methodology to obtain better accuracy.

6. REFERENCES

[1] Koko, T.S., Gallant, B.K. and Tobin, S.M. "Investigation of Plastic Zone Development in Dynamic Tear Test Specimens." DREA, Contractor Report DREA-1999-095 July 1999.

[2] Koko, T.S., Gallant, B.K. and Tobin, S.M. "Investigation of Plastic Zone Development in Dynamic Tear Test Specimens – Phase II." DREA, Contractor Report DREA-CR2000-115 September 2000.

[3] Hibbitt, H.D. Karlsson, B.I. and Sorensen, E.P. ABAQUS User's Manual, 1990.

[4] Matthews, J.R. "On the Relationship between Shear Lip, Shear Index and Energy in Dynamic Tear Specimens", Engineering Fracture Mechanics, Vol. 54, No. 1, pp. 11-23, 1996.

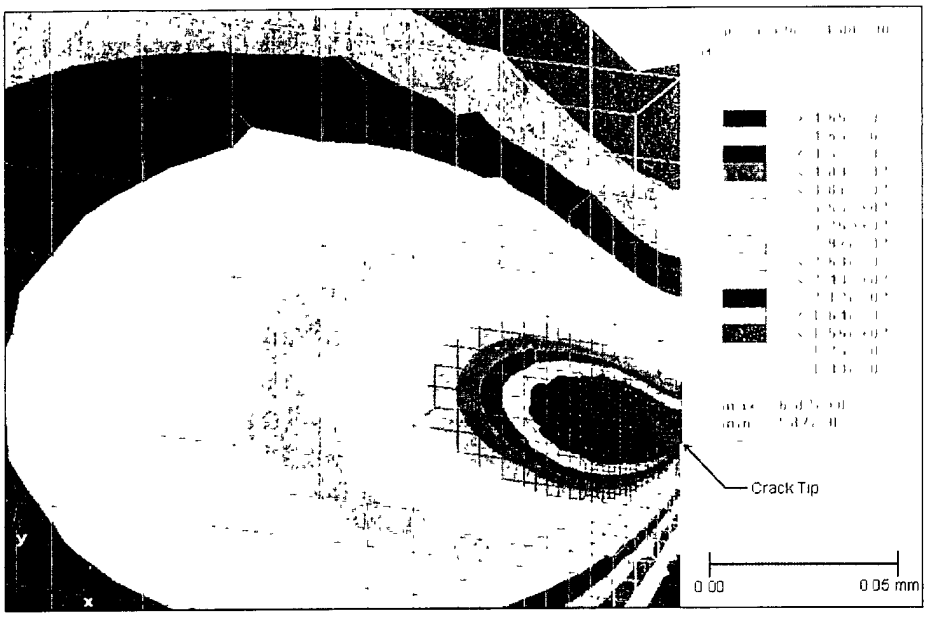

(a)

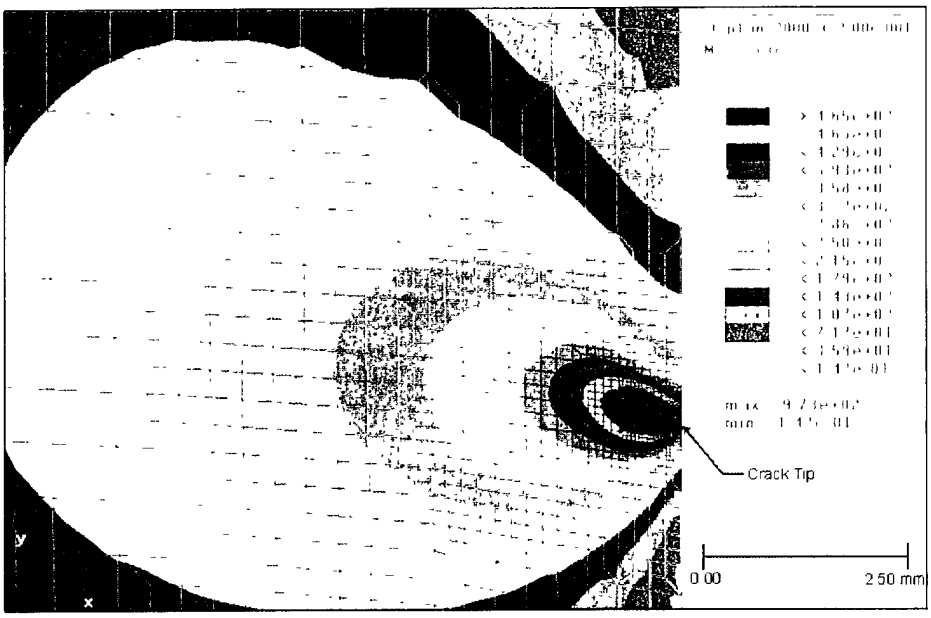

(b)

Figure A.1: von Mises Stress Contours in DT-350WT-08 Specimen Using Mesh 1Q
(a) D_L / B = 0.00542 (b) D_L/B = 0.02718

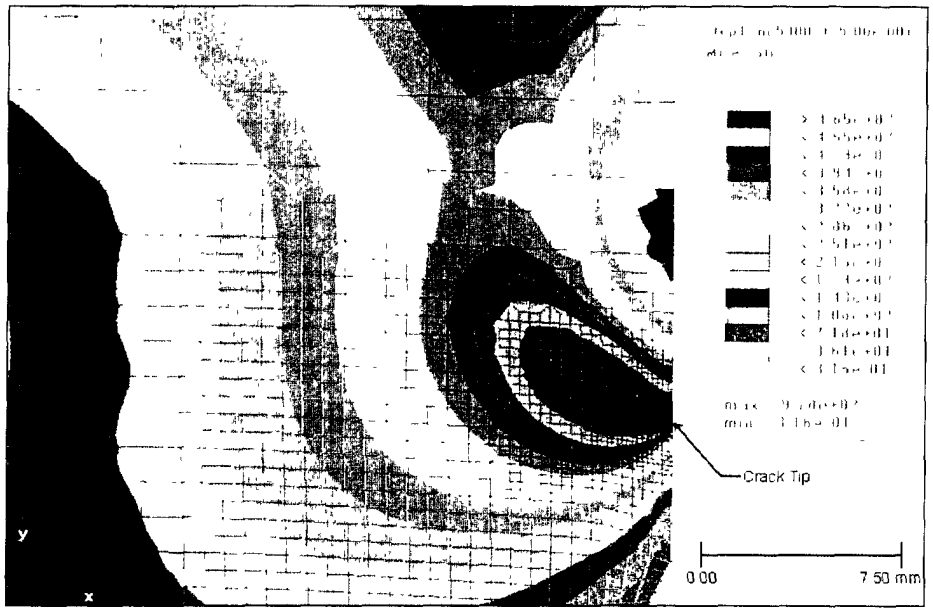

(c)

Figure A.1: von Mises Stress Contours in DT-350WT-08 Specimen Using Mesh 1Q
(c) $D_L/B = 0.06991$

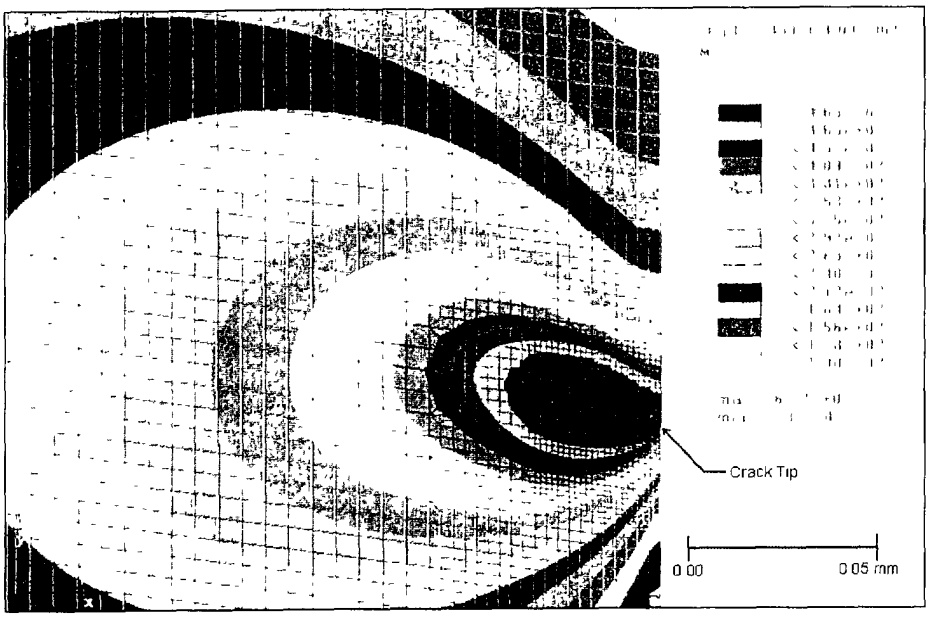

(a)

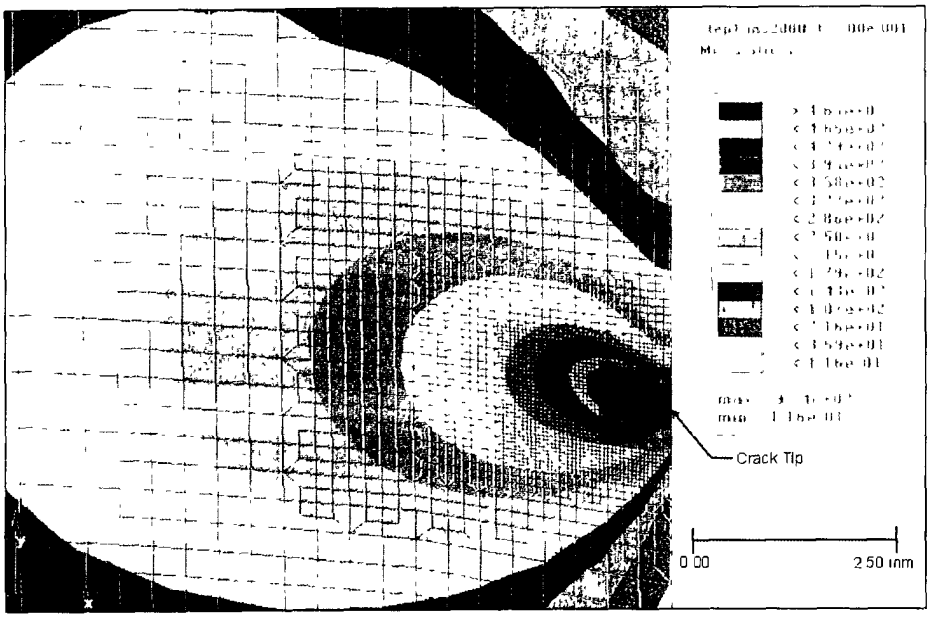

(b)

Figure A.2: von Mises Stress Contours in DT-350WT-08 Specimen Using Mesh 2L
(a) D_L / B = 0.00543 (b) D_L/B = 0.02720

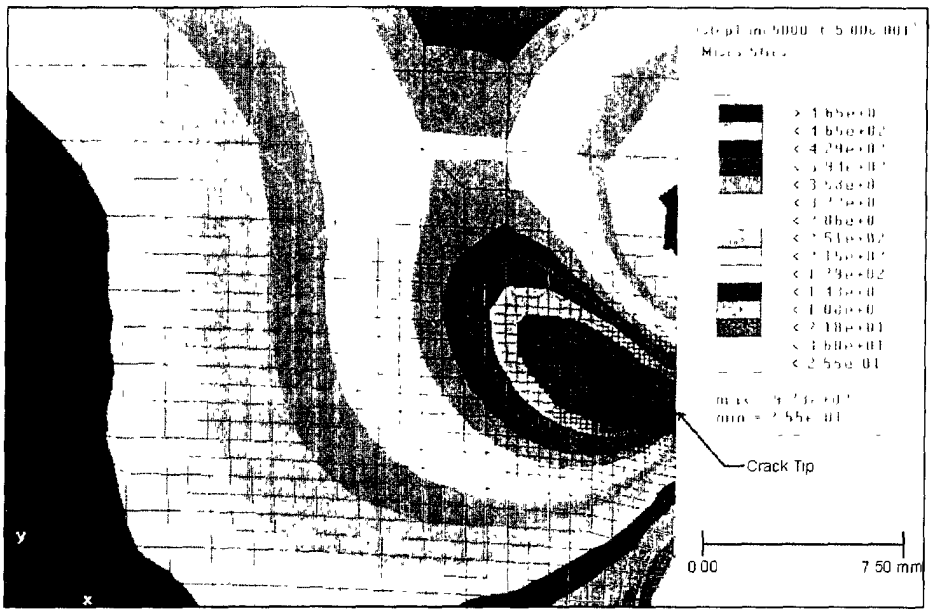

(c)

Figure A.2: von Mises Stress Contours in DT-350WT-08 Specimen Using Mesh 2L
(c) $D_L/B = 0.06944$

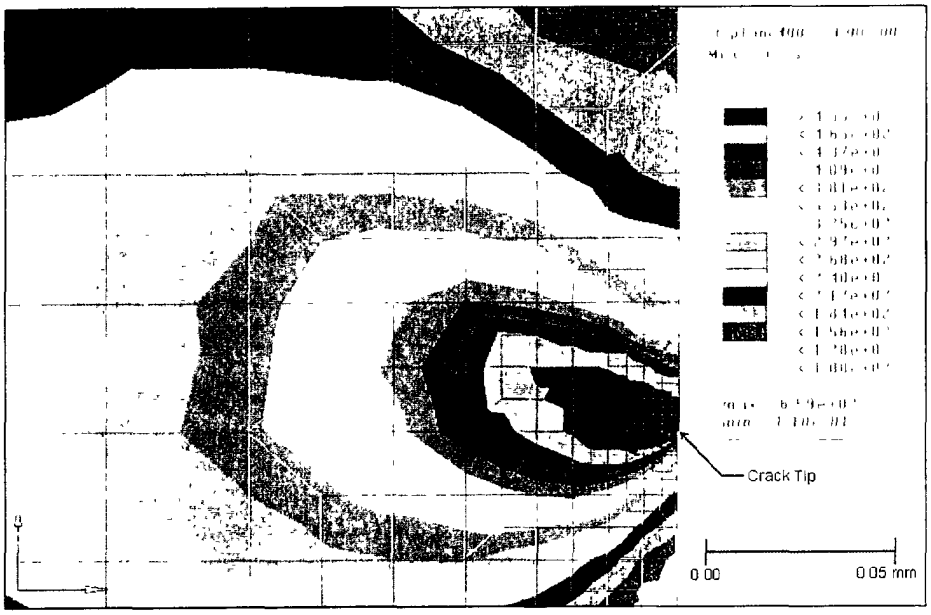

(a)

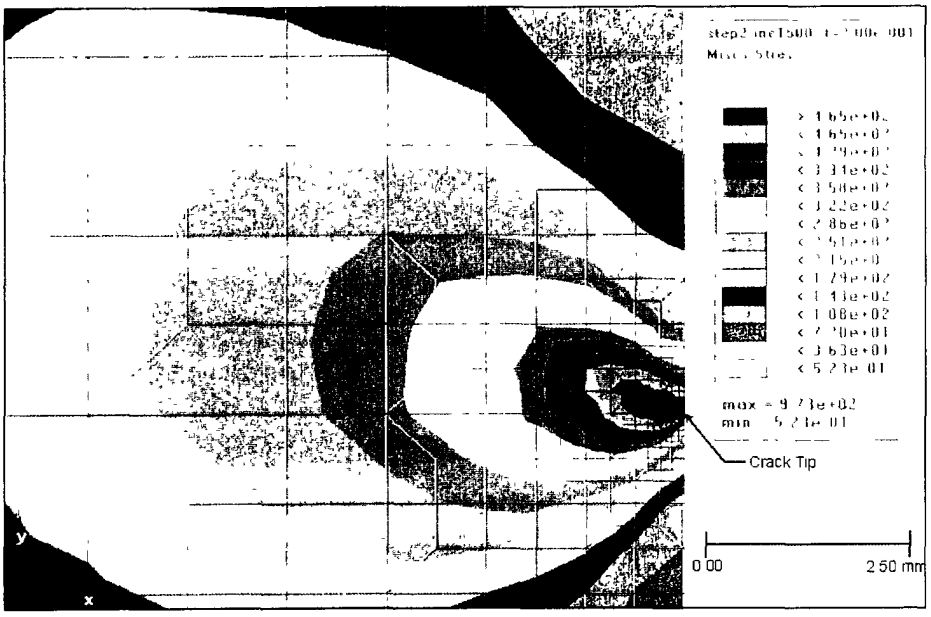

(b)

Figure A.3: von Mises Stress Contours in DT-350WT-08 Specimen Using Mesh 3L
(a) D_L / B = 0.00546 (b) D_L/B = 0.02634

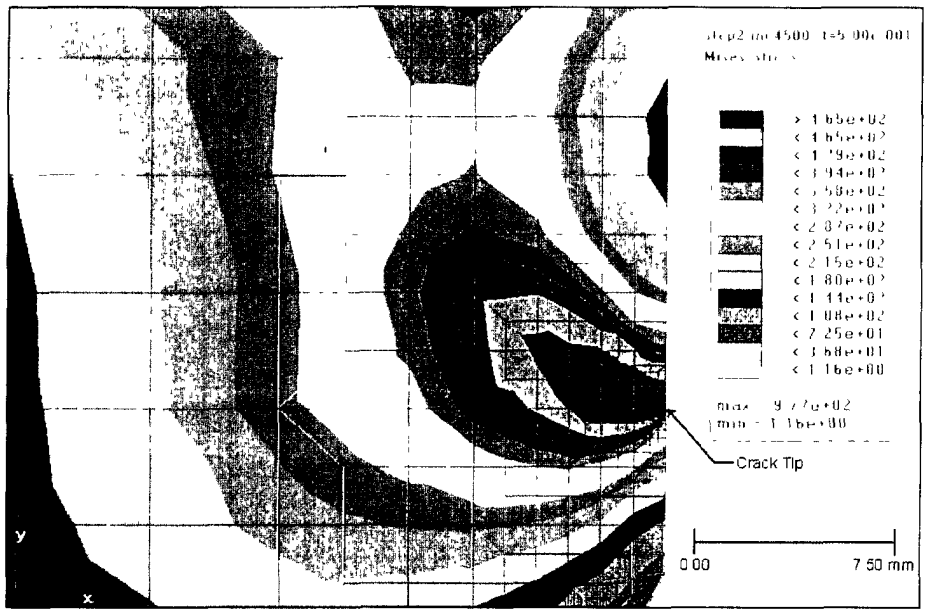

(c)

Figure A.3: von Mises Stress Contours in DT-350WT-08 Specimen Using Mesh 3L
(c) $D_L/B = 0.06372$

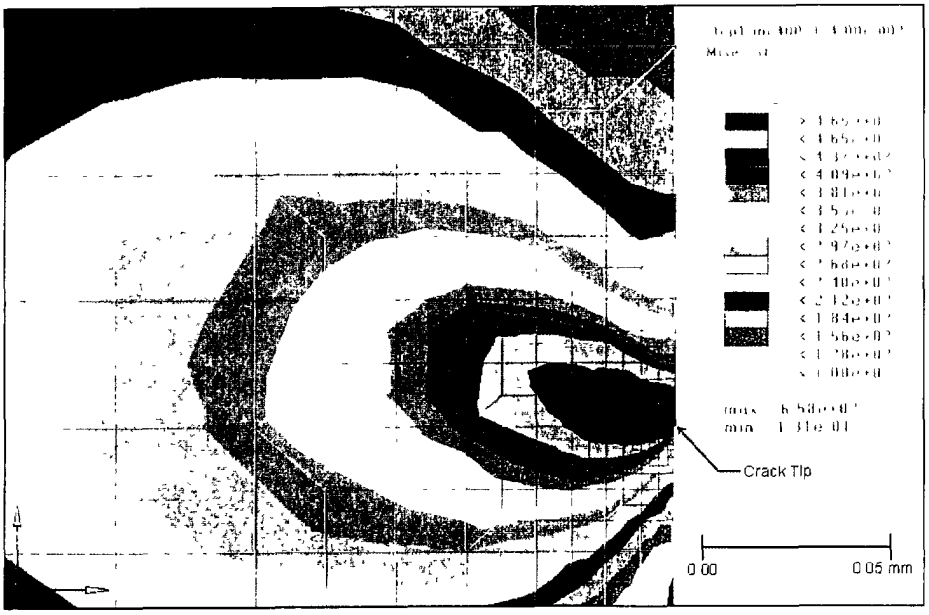

(a)

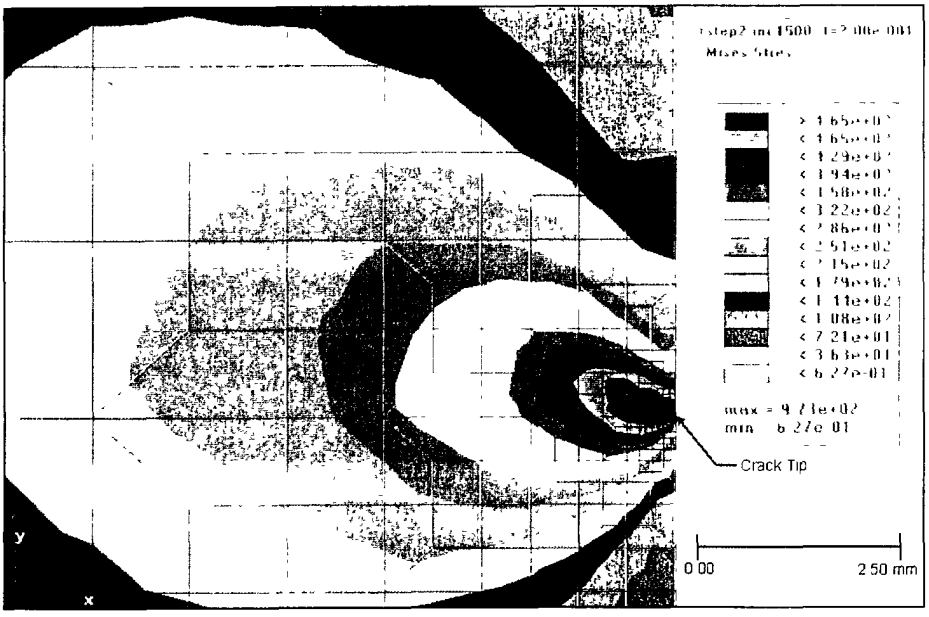

(b)

Figure A.4: von Mises Stress Contours in DT-350WT-08 Specimen Using Mesh 3Q
(a) D_L / B = 0.00544 (b) D_L/B = 0.02580

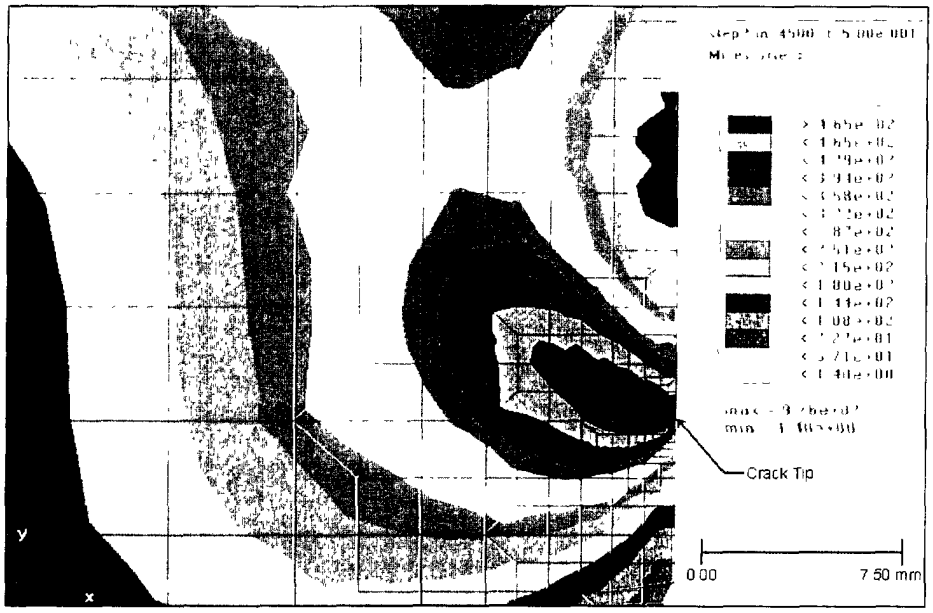

(c)

Figure A.4: von Mises Stress Contours in DT-350WT-08 Specimen Using Mesh 3Q
(c) $D_L/B = 0.06436$

UNCLASSIFIED
SECURITY CLASSIFICATION OF FORM
(highest classification of Title, Abstract, Keywords)

DOCUMENT CONTROL DATA

(Security classification of title, body of abstract and indexing annotation must be entered when the overall document is classified)

1 ORIGINATOR (the name and address of the organization preparing the document Organizations for whom the document was prepared, e g Establishment sponsoring a contractor's report, or tasking agency, are entered in section 8)

Martec Limited
400-1888 Brunswick Street
Halifax, NS, B3J 3J8

2 SECURITY CLASSIFICATION (overall security classification of the document including special warning terms if applicable)

UNCLASSIFIED

3 TITLE (the complete document title as indicated on the title page Its classification should be indicated by the appropriate abbreviation (S,C,R or U) in parentheses after the title)

Investigation of Plastic Zone Development in Dynamic Tear Test Specimens-Phase III

4 AUTHORS (Last name, first name, middle initial If military, show rank, e g Doe, Maj John E)

T.S. Koko and B.K. Gallant

5 DATE OF PUBLICATION (month and year of publication of document)	6a NO OF PAGES (total containing information Include Annexes, Appendices, etc)	6b NO OF REFS (total cited in document)
September 2001	52 (approx.)	4

7 DESCRIPTIVE NOTES (the category of the document, e g technical report, technical note or memorandum If appropriate, enter the type of report, e g interim, progress, summary, annual or final Give the inclusive dates when a specific reporting period is covered)

CONTRACTOR REPORT

8 SPONSORING ACTIVITY (the name of the department project office or laboratory sponsoring the research and development Include address)

Defence Research Establishment Atlantic
PO Box 1012
Dartmouth, NS, Canada B2Y 3Z7

9a PROJECT OR GRANT NO (if appropriate, the applicable research and development project or grant number under which the document was written Please specify whether project or grant)	9b CONTRACT NO (if appropriate, the applicable number under which the document was written)
Project 11GH 36	W7707-0-8440

10a ORIGINATOR'S DOCUMENT NUMBER (the official document number by which the document is identified by the originating activity This number must be unique to this document)	10b OTHER DOCUMENT NOs (Any other numbers which may be assigned this document either by the originator or by the sponsor)
	DREA CR 2001-121

11 DOCUMENT AVAILABILITY (any limitations on further dissemination of the document, other than those imposed by security classification)

(X) Unlimited distribution
( ) Defence departments and defence contractors; further distribution only as approved
( ) Defence departments and Canadian defence contractors; further distribution only as approved
( ) Government departments and agencies; further distribution only as approved
( ) Defence departments, further distribution only as approved
( ) Other (please specify)

12 DOCUMENT ANNOUNCEMENT (any limitation to the bibliographic announcement of this document This will normally correspond to the Document Availability (11) However, where further distribution (beyond the audience specified in (11) is possible, a wider announcement audience may be selected)

UNCLASSIFIED
SECURITY CLASSIFICATION OF FORM

UNCLASSIFIED
SECURITY CLASSIFICATION OF FORM
(highest classification of Title, Abstract, Keywords)

13. ABSTRACT (a brief and factual summary of the document It may also appear elsewhere in the body of the document itself It is highly desirable that the abstract of classified documents be unclassified Each paragraph of the abstract shall begin with an indication of the security classification of the information in the paragraph (unless the document itself is unclassified) represented as (S), (C), (R), or (U) It is not necessary to include here abstracts in both official languages unless the text is bilingual)

This study is a continuation of efforts to investigate plastic zone development in three-point bend fracture specimens to provide an understanding of crack tip blunting (stretch zone) to plastic zone size (radius), in order to be able to predict the upper limit where elastic plastic fracture becomes invalid. Finite element analyses of an 8mm specimen made of 350WT steel were performed with the aim of investigating the effects of various modeling (mesh) parameters on the behaviour of 2-D finite element models; and 3-D modeling to investigate shear lip behaviour. The ABAQUS finite element code was used to perform incremental elastic-plastic analysis of the specimens. The results computed included the progression of plastic strain, plastic radius (r_y), stretch zone width (SZW), and the r_y/SZW ratio with plastic displacement. It was found that the plastic radius and maximum plastic strains were not too sensitive to the mesh size around the crack tip, whereas the SZW is highly sensitive to mesh size around the crack tip. Thus the r_y/SZW ratio also depends on mesh configuration. In creating meshes around the tip, it is necessary to ensure that the sizes of the elements around the tip are such that several elements are contained in the region from the crack tip to the side of the crack where the yield line intersects the side of the crack. The 3-D analyses confirmed the in-plane plastic zone patterns obtained from the 2-D analyses and provided some insight on the shear lip behaviour. However, the results obtained from the analyses did not provide a distinct point at which to measure the shear lip. At a plastic displacement of 0.0975B (B = specimen thickness) the shear index was estimated to be 0.6 at the point where the yield lines were closest. Further studies are required to provide more accurate estimates of the shear lip size.

14 KEYWORDS, DESCRIPTORS or IDENTIFIERS (technically meaningful terms or short phrases that characterize a document and could be helpful in cataloguing the document They should be selected so that no security classification is required Identifiers, such as equipment model designation, trade name, military project code name, geographic location may also be included If possible keywords should be selected from a published thesaurus e g Thesaurus of Engineering and Scientific Terms (TEST) and that thesaurus-identified If it not possible to select indexing terms which are Unclassified, the classification of each should be indicated as with the title)

plastic zone
stretch zone width
finite element
ABAQUS

UNCLASSIFIED
SECURITY CLASSIFICATION OF FORM

Defence R&D Canada
is the national authority for providing
Science and Technology (S&T) leadership
in the advancement and maintenance
of Canada's defence capabilities.

R et D pour la défense Canada
est responsable, au niveau national, pour
les sciences et la technologie (S et T)
au service de l'avancement et du maintien des
capacités de défense du Canada.

DEFENCE R&D DÉFENSE

www.drdc-rddc.dnd.ca